

**NASA  
Technical  
Paper  
2122**

December 1983

**Simulator Study of Pilot-  
Aircraft-Display System  
Response Obtained With  
a Three-Dimensional-Box  
Pictorial Display**

James J. Adams

**LOAN COPY. RETURN TO  
AFWL TECHNICAL LIBRARY  
KIRTLAND AFB, N.M. 87117**

NASA  
TP  
2122  
c.1



25th Anniversary  
1958-1983

**NASA  
Technical  
Paper  
2122**

1983

TECH LIBRARY KAFB, NM



0134997

**Simulator Study of Pilot-  
Aircraft-Display System  
Response Obtained With  
a Three-Dimensional-Box  
Pictorial Display**

**James J. Adams**

*Langley Research Center  
Hampton, Virginia*



National Aeronautics  
and Space Administration

**Scientific and Technical  
Information Branch**

1983



## SUMMARY

A simulator study of the use of a pictorial aircraft-guidance display has been conducted. The display presents a drawing of a three-dimensional box that is located on the desired path and moves along that path ahead of the aircraft. The simulator modeled a typical four-place, single-engine, high-wing aircraft, and position-regulation tasks were performed. The purpose of the study was to examine the effect on the pilot-aircraft-display system response of varying the field of view and distance to the box, both of which are design parameters of the display. Pilot rankings, system performance, and system-response characteristics were determined.

The pilots preferred the display configuration that used distances to the box of 368 m (1200 ft) and 915 m (3000 ft) and a field of view of  $\pm 30^\circ$ . Shorter distances resulted in higher system frequencies and longer distances resulted in lower system frequencies, both of which the pilots preferred less. Fields of view larger or smaller than  $\pm 30^\circ$  resulted in less system damping, which the pilots preferred less.

The best performance, both in the sense of quickness of error correction and lower standard deviations of lateral- and vertical-position errors, was obtained with a short distance to the box of 92 m (300 ft) and a field of view of  $\pm 15^\circ$ . With a narrower field of view of  $\pm 5^\circ$ , the system damping was so low that performance was adversely affected. Longer distances to the box resulted in lower system frequencies, slow system response, and large errors.

## INTRODUCTION

The "follow me" box pictorial display is an aircraft-guidance display that combines many potential advantages in a very simple drawing, which can be implemented with an onboard digital computer, a cathode-ray-tube display device, and standard aircraft navigation and attitude sensors. The display presents a drawing of a three-dimensional box that is located on the desired path and moves along the path ahead of the aircraft. The box symbol provides sufficient information on position errors and attitude angles for the pilot to position the aircraft on the desired path. The different features of the symbols (its shape and location in the display) present the different variables independently so that, in particular, displacement errors are shown independently. The pilot's task is simply to follow the box.

Because of these features of the "follow me" box display, it has been shown in previous studies that the pilot-aircraft-display system can be operated at a much higher frequency than that obtained with either conventional displays or flight-director displays. The result of the higher system frequency is more precise control of aircraft position. These previous studies (refs. 1 to 5) have shown that although very precise control can be obtained with the box display, this benefit is tempered by the fact that the pilots note an increase in work load when the parameters of the display are adjusted to provide precise control as compared to when they are adjusted to provide less-precise control. The studies of references 1, 3, and 4 show that a trade-off is possible between precision of control and work load by varying the distance to the box. Also, in reference 1 a field of view of  $\pm 25^\circ$  was used because this

field of view was found to be very comfortable. In reference 3 a field of view of  $\pm 45^\circ$  (in the lateral direction) was used because of a desire to have a field of view as large as practical for en route navigation.

The purpose of the present study is to examine variations in distance to the box and field of view in more detail than the previous studies. The effects of varying the field of view from  $\pm 5^\circ$  to  $\pm 45^\circ$  and the distance to the box from 92 m (300 ft) to 6100 m (20 000 ft) are examined. Seven instrument-rated subjects with varying amounts of flying experience gave their rankings and comments on the use of the display. Performance data and characteristics of pilot-aircraft-display system response were measured. The results of this study can be compared directly with results for conventional displays (ref. 2) and flight-director displays (ref. 5) because the same simulator, aircraft model, wind disturbance, and general test format were used in each study. The simulator modeled a typical four-place, single-engine, high-wing aircraft. The tasks which the pilots executed were simple laboratory-type position-regulating tasks with initial errors or in the presence of winds and gusts. The results should be applicable to general aviation type aircraft.

#### SYMBOLS

Values are given in SI Units and, where considered useful, also in U.S. Customary Units. Measurements and calculations were made in U.S. Customary Units.

$G_u, G_v, G_w$	gust spectrum transfer functions
$g$	acceleration due to gravity, $\text{m/sec}^2$ ( $1g = 9.8 \text{ m/sec}^2$ )
$h$	altitude, m
$K_h, K_y$	pilot-model gains, rad/m
$K_\theta, K_\psi, K_\phi$	dimensionless pilot-model gains
$L_u, L_v, L_w$	gust characteristic wavelengths, m
$p, q, r$	roll, pitch, and yaw angular rates, respectively, rad/sec
$s$	Laplace operator, $\text{sec}^{-1}$
$u_g, v_g, w_g$	orthogonal random gust components, m/sec
$V$	aircraft velocity, m/sec
$X, Y, Z$	aircraft body-axis system
$X_i, Y_i, Z_i$	inertial axes
$x_{iA}, y_{iA}, z_{iA}$	aircraft inertial position, m
$x_{iB}, y_{iB}, z_{iB}$	box inertial position, m
$y$	lateral displacement, m

# ***Error***

---

An error occurred while processing this page. See the system log for more details.

## DESCRIPTION OF EXPERIMENT

The purpose of this experiment was to examine the effect on pilot-aircraft-display system response of variations in distance to the box in the direction of the desired path (Dist.) and field of view (FOV). The matrix of values examined, together with the number identifying the configuration, is given in the following table:

Configuration Number					
Distance to box		Field of view of -			
m	ft	$\pm 5^\circ$	$\pm 15^\circ$	$\pm 30^\circ$	$\pm 45^\circ$
92	300	1	2	3	4
184	600	5	6	7	8
368	1 200	9	10	11	12
915	3 000			13	
6100	20 000			14	

A discussion of the display concept that will help in understanding the role of the experimental parameters will be given in the following sections. Also given is a description of other important factors such as the simulator and aircraft model, the wind disturbances, the flight experience of the subjects, the test procedures, and a description of the pilot-model analysis of the pilot-aircraft-display system response.

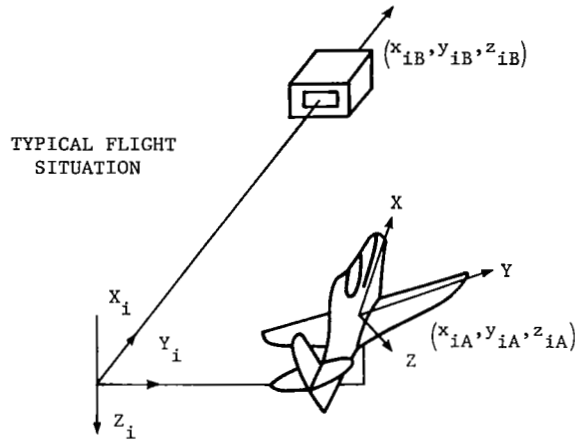
### Display Concept

Sketch A shows a typical flight situation in which the aircraft, banked to the left, is to the right and above the desired path. The display for this typical flight situation is shown in sketch B.

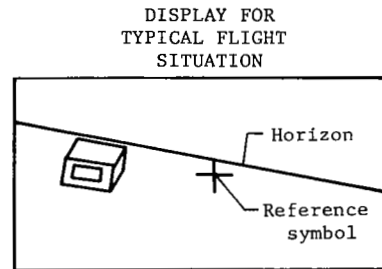
To illustrate the information content of the display, consider the simplified lateral situations shown in sketch C. A heading error alone (no displacement error) results in the display shown on the left with the box displaced from the aircraft reference symbol. A displacement error alone (no heading error) also causes the box to be displaced from the reference symbol, but with the side of the box visible. (See right side of sketch C.) Placing the aircraft reference symbol on the near face of the box results in a heading angle that will eliminate the displacement error in time. As the displacement error is reduced, the side of the box disappears. Thus, both quickened data (a combination of displacement and rate of change of displacement) and raw displacement data are provided by the display.

The algorithm for drawing the box is presented in references 1 and 3. The inputs required to draw the box are the orthogonal distances  $x_{iB} - x_{iA}$ ,  $y_{iB} - y_{iA}$ , and  $z_{iB} - z_{iA}$ , the measured attitudes of the aircraft, and selected values for the field of view and for the size and attitudes of the box. It is assumed that the distances of the aircraft from the desired path,  $y_{iB} - y_{iA}$  and  $z_{iB} - z_{iA}$ , are obtained from the navigation system. The other distance required,  $x_{iB} - x_{iA}$ , is a

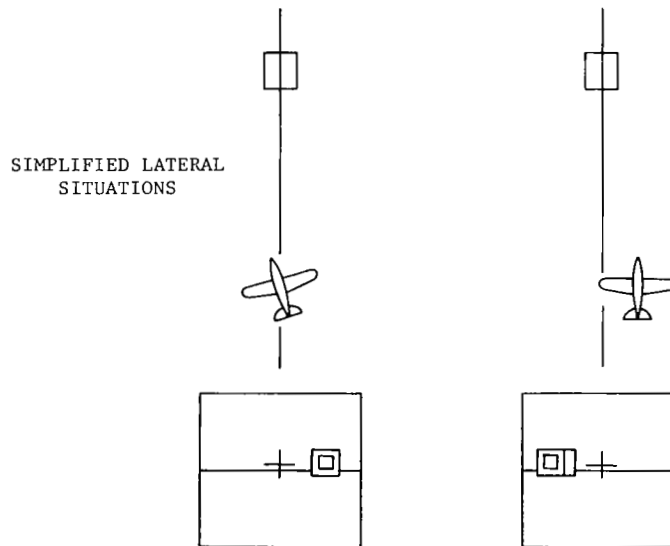
selected value and determines the displacement sensitivity of the display. With an  $x_{iB} - x_{iA}$  value of 92 m (300 ft) and a lateral error of 10 m (33 ft), the box would be seen at an angle of  $6.2^\circ$ . With an  $x_{iB} - x_{iA}$  value of 915 m (3000 ft) and a lateral error of 10 m (33 ft), the box would be seen at an angle of  $0.6^\circ$ . In this manner, the distance to the box changes the displacement sensitivity of the display.



Sketch A



Sketch B



Sketch C

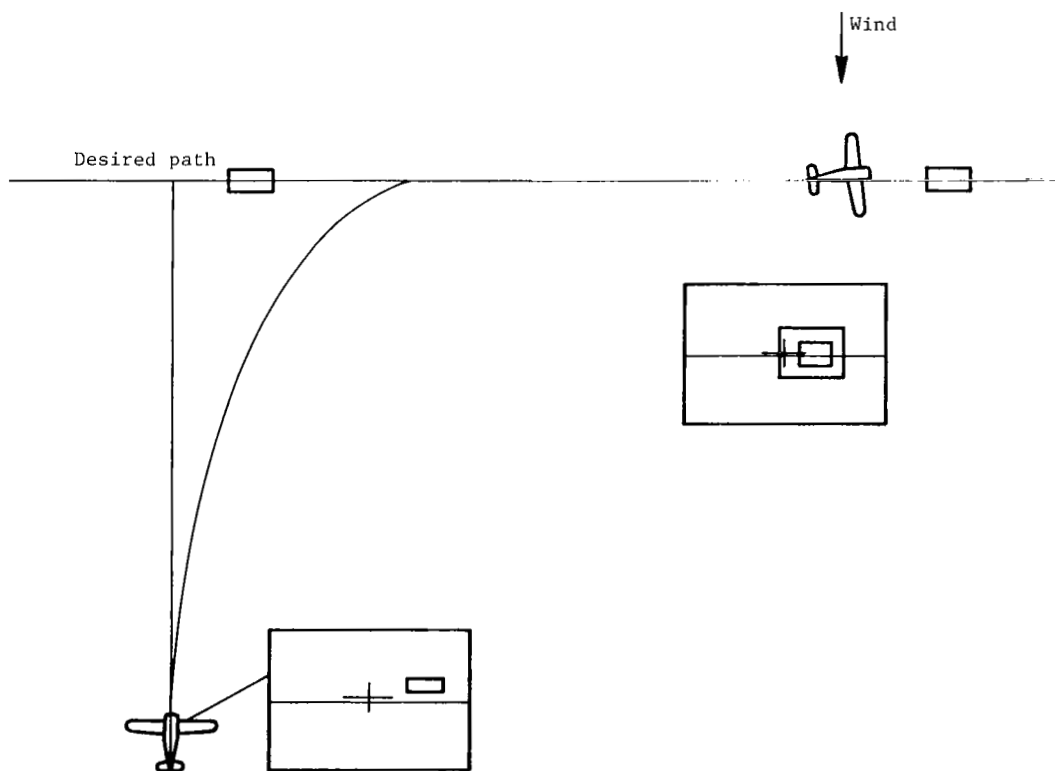
The field of view has a direct effect on the heading- and pitch-angle sensitivity of the display. With a field of view of  $\pm 5^\circ$  and no displacement error, a heading change of  $5^\circ$  would move the box to the edge of the display. With a  $\pm 45^\circ$  field of view, a heading change of  $45^\circ$  would be required to move the box to the edge of the display. In this manner, the selected field of view governs the heading- and pitch-angle sensitivity of the display.



It should be pointed out that the box-drawing algorithm utilizes techniques that result in the drawing of only those edges of the box that would be visible to the pilot. These hidden-line masking techniques eliminate the confusion that would exist if they were not used. The algorithm also results in the box being drawn with parallel sides, as opposed to other techniques that could be used that would result in a vanishing-point type of perspective. The result is that when the aircraft is 0.3 m (1 ft) to the left of the desired path, a double line is drawn on the left side of the box to show the left side of the box. When the aircraft is 0.3 m to the right of the desired path, a double line is drawn on the right side of the box. This drawing technique, therefore, provides a very sensitive indication of small displacement errors, which would not be present if a vanishing-point perspective were used.

Although the display can present a very sensitive indication of position error, it can also provide a useful signal when the aircraft is very far from the desired path. This situation is illustrated in sketch D, which shows both how the display will look when the lateral error is very large (see left side) and how it will look when the error is small (see right side). The subjects were told that pointing at the box would reduce the position error. They were also told that when the errors were small, and in the presence of winds and longitudinal trim changes, it would be necessary to adjust the aim point slightly. This situation is also illustrated in sketch D, which shows the aim point at the left of the box to compensate for the crosswind from the left.

TYPICAL FLIGHT SITUATION  
WITH DISPLAY



Sketch D

## Simulator

By using six-degree-of-freedom nonlinear equations of motion, the simulator modeled a typical four-place, single-engine, high-wing general aviation aircraft. In addition to nonlinear kinematics, the following nonlinear aerodynamics factors and other special features were included in the simulation:

- (1) Nonlinear lift and drag coefficients were a function of  $\alpha^2$  as well as of  $\alpha$ .
- (2) Nondimensional stability coefficients  $C_{Y\beta}$ ,  $C_{L\delta e}$ ,  $C_{l\beta}$ ,  $C_{n\delta a}$ , and  $C_{n\beta}$  were a function of  $\alpha$ .
- (3) Asymmetric forces and moments as a function of thrust coefficient were included.
- (4) A hydraulic control loader provided forces as a function of the aerodynamic hinge moment.
- (5) A sound system provided realistic engine and airstream noise.

The dynamic response of the simulator aircraft model to control step inputs at the nominal test airspeed (85 knots) is shown in figure 1. Figure 1(a) shows the short-period longitudinal response to a 0.02-rad elevator step input. The response is well-damped with a frequency of 2 rad/sec. The phugoid response is shown in figure 1(b) and is fairly well-damped with a period of 30 sec. The lateral response (fig. 1(c)) is also fairly well-damped with a frequency of 2 rad/sec. Figure 1 also shows the undesirable large effect of the adverse yaw which was included in the aircraft model.

The display was presented on a 7.6-cm by 10.16-cm cathode-ray tube (CRT) mounted in the center of the instrument panel, as shown in figure 2. The CRT replaced the attitude indicator. The rest of the panel was left in a standard configuration.

The field-of-view size given in the experimental matrix refers to the lateral field of view; the vertical field of view was three-fourths that of the lateral field of view. The zero-pitch-angle location of the display was placed one-third of the distance down from the top of the display. The aircraft had a 4°-trim pitch angle at the nominal airspeed of the test. Therefore, with the  $\pm 5^\circ$  field of view, the horizon was one-third of the distance up from the bottom of the display at trim for a 1g flight. With the larger fields of view, the trim position of the horizon was more nearly at the center of the display.

## Test Procedures

Two types of tests were conducted in this study. In the first type, the test was started with the aircraft displaced from the desired path both vertically and laterally, and the pilot had to maneuver the aircraft onto the desired path. The command path was straight and level. The initial errors were sized so that the box always appeared in the upper right corner of the display, with the exception that the vertical error was never larger than 184 m (600 ft). Also, the size of the box was changed with each display configuration so that the box always subtended the same size on the display when the lateral and vertical errors were zero. The box

dimensions were always in the same ratio: Width = 2 × Height; Length = 2 × Width. The initial error and box width for sample test configurations are given in the following table:

Configuration	FOV, deg	Dist.	Box width		Initial lateral error		Initial vertical error	
			m	ft	m	ft	m	ft
3	±30	92	31.2	102	47.5	156	35	115
7	±30	184	62.3	204	95	312	69	226
9	±5	386	20.7	68	32	105	23	75
10	±15	386	62.3	204	95	312	69	226
11	±30	386	124.0	407	170	558	139	456
12	±45	386	187.0	614	286	938	184	603
13	±30	915	312.0	1020	475	1 560	184	603
14	±30	6100	2080.0	6824	3180	10 433	184	604

In addition to these unique parameters for each case, a change was made in the sensitivity of the lateral and vertical strip charts that were obtained in each test. This method of recording strip-chart data emphasizes the pilot-aircraft-display system stability, rather than performance.

In addition to the recorded strip charts, the subjects were also asked to rank the configuration by assigning a ranking of 1 for the best configuration and of 7 for the worst. The subjects were shown configuration 10 for their first test and were told to give a ranking of 4 for configuration 10. Then, they should rank all other configurations relative to this first test. The other configurations were then presented to the subjects in random order, with repeat tests being conducted for some configurations.

Since the task performed in this study was rather simple (step corrections), and since the purpose of getting the subjects to give rankings was solely to obtain relative rankings, no attempt was made to use the Cooper-Harper pilot-ranking scale. The rankings obtained in this study should not be interpreted as being Cooper-Harper ratings.

The subjects were asked to use the box symbol as a target when correcting errors and to set their full attention on keeping the errors small. In order of priorities, they were asked (1) to keep the vertical error small, (2) to keep the lateral errors small, and (3) to keep the airspeed at 85 knots. The subjects were asked to treat the task as though precise positioning of the aircraft was required, that is, to think of the task as a landing-approach task.

Following these tests with initial errors, the subjects were given a second series of tests in which the aircraft was started on the desired path and the subjects had to keep the aircraft on this path in the presence of crosswinds and gusts. Again, the configurations were presented in a random order. Standard deviations and

means of the lateral and vertical errors were obtained in these tests. The subjects were not asked for rankings of the display configurations when the gust inputs were used.

### Wind Inputs

In the tests in which wind inputs were used as forcing functions, these inputs consisted of a steady crosswind with a magnitude of 2.4 knots and a random input used to represent gusts which was based on the Dryden model. (See ref. 6.) Three gust inputs  $u_g$ ,  $v_g$ , and  $w_g$  were generated by using random-number generators and filters based on the Dryden gust model. The filter algorithms were

$$G_u(s) = \sigma_u \frac{1}{s + \frac{V}{L_u}}$$

$$G_v(s) = \sigma_v \frac{s + \frac{1}{\sqrt{3}} \frac{V}{L_v}}{\left(s + \frac{V}{L_v}\right)^2}$$

$$G_w(s) = \sigma_w \frac{s + \frac{1}{\sqrt{3}} \frac{V}{L_w}}{\left(s + \frac{V}{L_w}\right)^2}$$

The scale lengths were

$$L_u = L_v = h \quad (\text{for } h > 533 \text{ m (1750 ft)})$$

$$L_u = L_v = 44h^{1/3} \quad (\text{for } h < 533 \text{ m (1750 ft)})$$

$$L_w = h$$

The gust amplitudes were adjusted so that the root-mean-square value was 2.4 knots at an altitude of 533 m. The mean value of the gusts was zero.

### Subjects

Seven subjects took part in the tests, and all were instrument rated. Four subjects, who were engineers employed at the Langley Research Center, flew on an

occasional basis. Three subjects, who were experienced NASA test pilots, flew all types of aircraft on a regular basis. The age and accumulated flight hours of the subjects are listed in the following table:

Subject	Age	Flight hours	Experience
1	46	400	Very little IFR time; no flight-director time
2	27	1600	Conventional instruments only; no flight-director time
3	33	1600	300 hr flight-director time
4	37	2600	No flight-director flight time; 150 hr in simulators
5	41	4500	} Extensive experience
6	47	7500	
7	54	7300	

#### Pilot-Model Analysis Procedures

A servomechanism, multiloop pilot model was used to provide time histories that would match the time histories obtained from the subjects. These procedures were also used in references 1 and 2. This model matching determines the gains that the pilot used in his response to the display. The variations in pilot gains with display configurations provide a very useful insight into how the pilot used the display. This insight is further enhanced by determining the linear pilot-aircraft-display system characteristics. These system characteristics illustrate the effect of the pilot gains on the complete system.

The time histories were obtained by using the pilot model in conjunction with the nonlinear aircraft model. Variations in system response were obtained mainly by adjusting the linear gains in the pilot model. Some limiters were also included in the pilot model for making fine-tuning adjustments in the system response. A remnant term was also included in the output of the pilot model, with the amplitude of the remnant adjusted to a suitable value.

Once the time-history matches were obtained, the pilot-model gains determined were used in a linear version of the pilot model (leaving out the limiters) in combination with a linear version of the aircraft model to determine analytically the linear-system characteristics.

To illustrate the form of the pilot model and the nature of the multiloop pilot-aircraft system, a block diagram is presented in figure 3. This block diagram shows the pilot model, including the limiters that were put on the pitch, heading, and bank-angle commands, in combination with a linearized version of the aircraft. By using this diagram, it can be seen that the servomechanism pilot model hypothesizes that the pilot operates in the following manner. For lateral control, the model hypothesizes that the pilot observes the lateral-position error, multiplies the error by a factor  $K_y$ , and arrives at a desired value for heading angle. This sequence is assumed because a given heading angle will result in a given rate of change in position. The pilot may put an upper limit on this commanded value of heading angle. He then compares this desired value for heading angle with the actual heading of the

aircraft. If a difference exists, the pilot will multiply this heading error by a factor  $K_\psi$  and arrive at a desired value for bank angle. He does this because a given bank angle will result in a given rate of change in heading angle. The commanded bank angle is compared with the actual bank angle of the aircraft and, if a difference exists, the error is multiplied by a factor  $K_\phi$  to create a desired control deflection. The pilot then moves the control to match the commanded control value. A second-order lag is involved in making this control movement. A similar system is used to control vertical position.

In a multiloop system such as the aforementioned, the system-response stability characteristics are very much dependent on the ratios of the loop gains. To illustrate this interaction, consider the results presented for lateral control in the following table:

$K_y$ , rad/m	$K_\psi$	$K_\phi$	System stability
0.0033	1	-0.1	Unstable
.0033	1	-.2	Stable
.0066	1	-.2	Unstable
.0066	1	-.4	Stable
.0098	1.5	-.4	Unstable
.0098	2	-.6	Stable

These results were obtained by using the linear pilot model in combination with the nonlinear aircraft model. The pilot-model gains used fall within the normal range for pilots using instruments. It can be seen that the system changes from stable to unstable, depending on the combination of the gains. The system stability is not determined by any one gain alone.

It is also instructive to consider the changes in system-response characteristics that occur as the system loops are closed successively. Typical results are presented in the following table. These results were obtained by using the linear pilot model in combination with a linear version of the aircraft model. These linear systems, both vertical and lateral, are presented in the appendix.

With no control loops closed, the system-response characteristics are those of the basic aircraft. For lateral control, when the bank-angle loop is closed, a control mode is introduced that is derived from the second-order lag included in the pilot model, and the roll and spiral aircraft modes are moved to form an oscillatory mode of motion that is well-damped. When the heading loop is closed, a first-order heading mode is created, and the new oscillatory mode is reduced in damping and frequency. When the lateral-displacement loop is closed, a first-order displacement mode is created and the new oscillatory mode is reduced even further in damping. This oscillatory mode of motion is the dominant mode of the complete system response, and the reduction in damping that occurs when the lateral-displacement loop is closed is a potential source of difficulty. For vertical control, when the pitch and vertical-displacement loops are closed, a new oscillatory mode of motion is created which has low damping and is a potential source of difficulty.

Lateral linear system							
Pilot-model gains			Closed-loop system characteristics				
$K_y$ , rad/m	$K_\psi$	$K_\phi$	Control mode		Dutch roll mode		Roll, spiral, heading, and lateral modes
			$\omega_c$ , rad/sec	$\zeta_c$	$\omega_{DR}$ , rad/sec	$\zeta_{DR}$	
0	0	0			1.95	0.208	$\lambda_R = -4.94 \text{ sec}^{-1}$ ; $\lambda_S = -0.023 \text{ sec}^{-1}$ ; $\lambda_\psi = 0$ ; $\lambda_y = 0$
0	0	-.5	6.85	0.94	2.10	.19	$\omega = 1.22 \text{ rad/sec}$ ; $\zeta = 0.87$ ; $\lambda_\psi = 0$ ; $\lambda_y = 0$
0	1.5	-.5	6.75	.95	2.11	.17	$\omega = 0.58 \text{ rad/sec}$ ; $\zeta = 0.66$ ; $\lambda_\psi = 1.49 \text{ sec}^{-1}$ ; $\lambda_y = 0$
.0082	1.5	-.5	6.70	.95	2.19	.16	$\omega = 0.41 \text{ rad/sec}$ ; $\zeta = 0.14$ ; $\lambda_\psi = 1.27 \text{ sec}^{-1}$ ; $\lambda_y = -0.87 \text{ sec}^{-1}$

Vertical linear system						
Pilot-model gains		Closed-loop system characteristics				
$K_h$ , rad/m	$K_\theta$	Control mode		Short period		Pitch and altitude modes
		$\omega_c$ , rad/sec	$\zeta_c$	$\omega_{sp}$ , rad/sec	$\zeta_{sp}$	
0	0			2.01	0.555	$\lambda_\theta = 0$ ; $\lambda_h = 0$
0	-.2	5.16	0.99	1.95	.475	$\lambda_\theta = -1.52 \text{ sec}^{-1}$ ; $\lambda_h = 0$
.0098	-.2	5.19	.99	1.97	.48	$\omega_h = 0.256 \text{ rad/sec}$ ; $\zeta_h = 0.18$

The lateral- and vertical-displacement outer-loop gains are closely related to the distance to the box. For example, in the case of lateral control when  $K_y = 0.0082 \text{ rad/m}$ , if the aircraft were 10 m to the side of the desired path, a heading angle of 0.082 rad would be commanded. If the aircraft were at this heading angle, the centerline extended from the aircraft would intersect the desired path 122 m in front of the aircraft. If the box were located 122 m in front of the aircraft, and the pilot tried to point at the box, he would be using an outer-loop gain of 0.0082 rad/m. The distance to the box, therefore, has a strong influence on the outer-loop gain that the pilot uses. There is no similar geometric relationship for  $K_\psi$  and  $K_\phi$ ; however, they can be influenced by the sensitivity of the display. As was explained before, the field of view selected directly affects the heading sensitivity of the display. As far as bank angle is concerned, the desire to show a true

picture of bank angle sets the sensitivity of the bank-angle display. For vertical control, the distance to the box strongly influences the outer-loop vertical gain  $K_h$ , and the field of view sets the sensitivity of the pitch display.

A remnant term is also included in the pilot model to represent the noisy part of the pilot's output. This remnant is formed with the use of a random-number generator and a second-order filter that is the same as the second-order filter in the pilot model. This remnant term is used when matching the time histories obtained from the subjects.

To obtain the time histories that are shown later, it was necessary to provide some airspeed control. The required control was provided by the experimenter by using a simple switch that changed the thrust coefficient. This simple control sufficed for the purposes of the present investigation.

## RESULTS AND DISCUSSION

### Pilot Rankings

Each subject gave a ranking for the different display configurations at the conclusion of each test with initial errors. These rankings are presented in table I. Certain configurations were given repeated tests, and the repeated rankings are given in these tests. The rank ordering of the configurations by each subject is presented in table II.

The rankings for configurations 1 to 13 were given with the assumption that the task was a landing approach. Configuration 14, which involved a large incremental change in distance to the box, was ranked by some of the subjects with the qualification that the ranking was for an en route navigation task.

The repeated rankings were, for the most part, consistent. The largest differences in repeated rankings for any one configuration was 3, which occurred in three tests. In the other 25 tests with repeated rankings, the differences were less than 3.

The rank orderings of the rankings show the clear preference of the subjects for the longer distances (368 and 915 m) to the box, which are near the top of the list for most subjects. The shorter distances (92 and 184 m) are placed near the bottom of the list. The rank orderings also show the clear preference for the  $\pm 30^\circ$  field of view, which are placed at the top of the list. The narrow field of view ( $\pm 5^\circ$ ) occupies the bottom position, thus showing a strong dislike for these configurations by the pilots. The  $\pm 45^\circ$  and  $\pm 15^\circ$  fields of view occupy the middle rankings, with the preference going to the  $\pm 45^\circ$  test.

Configuration 14 must be considered a special case, and two subjects indicated that they did consider it special by giving it a good ranking with the qualification that the good ranking applied only for an en route task, not for a landing-approach task. Subject 5 gave a poor ranking for configuration 14 with the specification that the poor ranking applied for both an en route task and a landing approach. His objection to giving a good ranking for an en route task was that he wanted a wider field of view. The other four subjects gave poor rankings for configuration 14 with no qualification whatsoever.



## Position Errors

The standard deviations and means of the vertical and lateral errors, measured during runs in which gusts and crosswinds were applied to the aircraft, are shown in tables III through VI. Sample time histories obtained with subject 1 are shown in figure 4. The rank ordering of the averages for all subjects for each variable of each configuration are shown in table VII. No values are given for configuration 1 because only two subjects were able to keep the box symbol in view in these tests. However, the individual scores for these two subjects are given in tables III through VI.

The rank ordering of the configurations show that the best (lowest) standard deviations are obtained with the shortest distances to the box and the smallest fields of view. The bottom of the rank-ordering list is filled with the longest distances and largest fields of view. These results are almost directly opposed to the pilot-ranking results. Therefore, a design for an operating system using the box display will require some compromise with regard to pilot preference and performance, with required performance being introduced as an important factor.

The two cases where the pilot rankings did correlate with performance are the two extreme configurations (1 and 14). Configuration 1 is a case in which the pilot-aircraft-display system damping is so close to zero that most subjects were not able to keep the box symbol in the field of view when gusts were applied to the aircraft. Therefore, no scores are given for configuration 1. The assumption is that the configuration is unacceptable. It should also be pointed out that subject 4 was not able to keep the box in view with configuration 5. However, the other six subjects were able to do so and, therefore, an average score is given for configuration 5. This average is for the six subjects who were able to use the configuration. With configuration 14, poor performance was obtained and most subjects gave poor rankings. However, as was noted before, two subjects gave good rankings for configuration 14 with the qualification that it be considered only for en route tasks.

## System-Response Characteristics

Time histories obtained from five subjects of their response to initial errors are shown in figures 5 through 9. Figures 5 and 6 show in detail the responses obtained from subjects 1 and 5, respectively, for configurations 5 through 8. Only lateral and vertical errors are shown in figures 7 to 9. Data for five subjects are presented to show the range of responses obtained.

Figures 5 through 10 can be used to judge the different configurations from a servomechanism point of view. They show the quickness with which lateral and vertical errors can be corrected and also the damping of the system. These figures show that a desirable combination of system frequency, which defines the quickness of response, and damping is consistently obtained with the  $\pm 30^\circ$  field of view. With some subjects, the response obtained with the  $\pm 15^\circ$  field of view appears to be better, but with other subjects it is not. The response is always slow with the  $\pm 45^\circ$  field of view and, in many cases, it is also poorly damped. The damping is always poor with the  $\pm 5^\circ$  field of view. With regard to distance to the box, it can be seen that slow, low-frequency responses are obtained with a long distance to the box and that fast, high-frequency responses are obtained with a short distance to the box. The highest frequencies are obtained with the shortest distances ( $x_{iB} - x_{iA} = 92 \text{ m}$  (300 ft)). Frequencies as high as 0.6 rad/sec (a period of 10 sec) can be seen.

Certain selected cases were matched by using a servomechanism pilot model. The time histories obtained with the pilot model are shown in figure 10. The nonlinear aircraft model that was used in the piloted simulation was used in conjunction with the pilot model to obtain these time histories.

The approximate gains that the pilots used are determined by the pilot-model analysis. The data show that the displacement gains  $K_h$  and  $K_y$  generally decrease as the distance to the box increases. The gain  $K_h$  varies from high values in the range from 0.016 to 0.019 rad/m to low values in the range from 0.0098 to 0.0066 rad/m;  $K_y$  varies from a high value of 0.01 rad/m to a low value of 0.0016 rad/m. Examining the time histories shows that along with these changes in gain, the system responses change from a high frequency to a slow, overdamped response.

The display sensitivity for heading  $\psi$  and pitch  $\theta$  change with field of view. The display sensitivity is highest with a small field of view and lowest for a large field of view. The pilot-model gains for heading and pitch  $K_\psi$  and  $K_\theta$ , respectively, also change with field of view, but the relationship is not linear. The lowest gains occur when the field of view is largest ( $K_\theta = 0.2$  and  $K_\psi = 0.8$  or  $0.5$ ). These gains increase when the field of view is reduced to  $\pm 30^\circ$  ( $K_\theta = 0.4$  and  $K_\psi = 2.0$ ). As the field of view is reduced even further to  $\pm 15^\circ$  and  $\pm 5^\circ$ , the gains  $K_\theta$  and  $K_\psi$  either remain constant or drop off slightly.

The display sensitivity of bank angle is the same for each display configuration. The pilot gains for bank angle do not change very much. The bank-angle gain is the same ( $K_\phi = -0.5$ ) for all values of field of view examined with the pilot-model analysis. The bank-angle gain  $K_\phi$  did vary some with distance to the box (going from -0.7 to -0.4), but these changes are less than the changes noted for the other pilot-model gains. The bank-angle gains measured in this study are greater than those measured in tests with conventional displays. (See ref. 2.) In reference 2,  $K_\phi$  varied from -0.16 to -0.32. On the other hand, the values noted for  $K_\phi$  in this study are less than those obtained in single-loop control tasks, where larger gains were measured. (See ref. 7.)

Analytically determined system-response characteristics were also obtained and are presented in the following table. These linear-system characteristics were obtained by using a linear perturbation model of the aircraft in combination with the linear pilot model. The resulting systems are a sixth-order vertical system and an eighth-order lateral system.

These analytically derived system characteristics confirm the statement that was made earlier in discussions on time histories. For lateral control, the Dutch roll mode is not affected by the closures of the pilot loops. This is true for the aircraft used in this study, but it would not be true generally. The dominant roll-heading mode of motion has a high frequency when the short distance to the box is used (configuration 3;  $\omega = 0.47$  rad/sec) and a low frequency when the long distance to the box is used (configuration 13;  $\omega = 0.28$  rad/sec). As far as field of view is concerned, very good system frequency and damping is obtained when a field of view of  $\pm 30^\circ$  is used (configuration 7;  $\omega = 0.48$  rad/sec;  $\zeta = 0.33$ ). When the narrow field of view is used, the damping of the roll-heading mode is low (configuration 5;  $\zeta = 0.12$ ). When the wide field of view is used, the system frequency is low and the damping does not show any noticeable increase (configuration 8;  $\omega = 0.17$  rad/sec;  $\zeta = 0.24$ ).

Lateral linear system										
Configuration	FOV, deg	Dist.	Pilot-model gains			Closed-loop-system characteristics				Roll, heading, and lateral modes
			$K_y$ , rad/m	$K_\psi$	$K_\phi$	Control mode		Dutch roll mode		
						$\omega_C$ , rad/sec	$\zeta_C$	$\omega_{DR}$ , rad/sec	$\zeta_{DR}$	
5	$\pm 5$	184	0.0082	2	-0.5	6.7	0.95	2.09	0.17	$\omega = 0.49 \text{ rad/sec}; \zeta = 0.12;$ $\lambda_\psi = -1.5 \text{ sec}^{-1}; \lambda_y = -0.68 \text{ sec}^{-1}$
			.0082	1.5	-.5	6.7	.95	2.10	.17	$\omega = 0.41 \text{ rad/sec}; \zeta = 0.14;$ $\lambda_\psi = -1.3 \text{ sec}^{-1}; \lambda_y = -0.87 \text{ sec}^{-1}$
6	$\pm 15$	184	0.0033	1.5	-0.5	6.7	0.95	2.10	0.17	$\omega = 0.37 \text{ rad/sec}; \zeta = 0.62;$ $\lambda_\psi = -1.4 \text{ sec}^{-1}; \lambda_y = -0.37 \text{ sec}^{-1}$
7	$\pm 30$	184	0.0066	2	-0.5	6.7	0.95	2.10	0.17	$\omega = 0.48 \text{ rad/sec}; \zeta = 0.21;$ $\lambda_\psi = -1.5 \text{ sec}^{-1}; \lambda_y = -0.56 \text{ sec}^{-1}$
			.0047	2	-.5	6.7	.95	2.09	.17	$\omega = 0.48 \text{ rad/sec}; \zeta = 0.33;$ $\lambda_\psi = -1.7 \text{ sec}^{-1}; \lambda_y = -0.41 \text{ sec}^{-1}$
8	$\pm 45$	184	0.0049	0.5	-0.5	6.7	0.95	2.12	0.18	$\omega = 0.17 \text{ rad/sec}; \zeta = 0.24;$ $\omega = 1.15 \text{ rad/sec}; \zeta = 0.91$
			.0033	.8	-.5	6.7	.96	2.01	.10	$\omega = 0.19 \text{ rad/sec}; \zeta = 0.45;$ $\omega = 1.04 \text{ rad/sec}; \zeta = 0.94$
3	$\pm 30$	92	0.0115	1.5	-0.7	6.9	0.95	2.19	0.15	$\omega = 0.47 \text{ rad/sec}; \zeta = 0.13;$ $\omega = 1.19 \text{ rad/sec}; \zeta = 0.78$
			.0082	1.5	-.7	6.9	.95	2.18	.15	$\omega = 0.42 \text{ rad/sec}; \zeta = 0.27;$ $\omega = 1.18 \text{ rad/sec}; \zeta = 0.74$
11	$\pm 30$	386	0.0049	1	-0.4	6.6	0.95	2.07	0.19	$\omega = 0.26 \text{ rad/sec}; \zeta = 0.26;$ $\lambda_\psi = -1.7 \text{ sec}^{-1}; \lambda_y = -0.54 \text{ sec}^{-1}$
13	$\pm 30$	914	0.00164	1	-0.4	6.6	0.95	2.07	0.19	$\omega = 0.28 \text{ rad/sec}; \zeta = 0.89;$ $\lambda_\psi = -1.7 \text{ sec}^{-1}; \lambda_y = -0.15 \text{ sec}^{-1}$

Vertical linear system										
Configuration	FOV, deg	Dist.	Pilot-model gains		Closed-loop-system characteristics				Pitch-altitude mode	
			$K_h$ , rad/m	$K_\theta$	Control mode		Short-period mode			
					$\omega_c$ , rad/sec	$\zeta_c$	$\omega_{sp}$ , rad/sec	$\zeta_{sp}$	$\omega_h$ , rad/sec	$\zeta_h$
5	$\pm 5$	184	0.0097 .0097	-0.4 -.2	5.3 5.2	0.98 .99	1.96 1.97	0.41 .48	0.35 .26	0.28 .18
6	$\pm 15$	184	0.0196 .0196	-0.6 -.4	5.5 5.4	0.97 .98	1.97 1.96	0.37 .43	0.59 .65	0.12 .065
7	$\pm 30$	184	0.0097	-0.4	5.3	0.98	1.95	0.41	0.35	0.27
8	$\pm 45$	184	0.0066	-0.2	5.3	0.97	1.97	0.48	0.21	0.27
3	$\pm 30$	92	0.0164 .0164	-0.32 -.24	5.2 5.3	0.98 .98	1.97 1.97	0.48 .45	0.35 .41	0.09 .11
11	$\pm 30$	386	0.0098	-0.4	5.3	0.98	1.95	0.41	0.35	0.27
13	$\pm 30$	914	0.0098	-0.32	5.3	0.98	1.96	0.44	0.32	0.24

For vertical control, the short-period mode is not affected by the pilot-loop closures. The pitch-altitude mode is affected, but to a much smaller degree than the lateral responses. Very good frequency and damping are obtained with the middle distances to the box and the  $\pm 30^\circ$  field of view (configuration 7;  $\omega = 0.35$  rad/sec;  $\zeta = 0.27$ ). When the short distance to the box is used, the pitch-altitude mode has low damping (configuration 3;  $\omega = 0.35$  rad/sec;  $\zeta = 0.09$ ).

In the context of this experiment, which does not involve a full, realistic task, the pilot rankings express the subject pilots' feelings about the dynamic-response characteristics of the pilot-aircraft-display system. When the rankings show a preference for configurations 11 and 13, the pilots are saying that they prefer the moderately slow, well-damped response obtained with these configurations. The pilots are able to use these configurations to arrive at system gains that result in these desirable response characteristics. However, the system gains are also influenced by the display sensitivities. Thus, with configuration 14, the very great distance to the box and the resulting extremely slow system response are disliked. Also, with short distances to the box and the resulting high system frequencies, poor subject rankings are obtained. As far as field of view is concerned, the system damping ratios in the range from 0.2 to 0.3 obtained with the  $\pm 30^\circ$  field of view are the preferred values. The heavily damped responses obtained with the very great distance to the box and the lower damping ratios obtained with the narrow and wide fields of view are not preferred.

System performance is also closely related to the system-response characteristics. The quickest error corrections are obtained with the high-frequency systems, and the lowest standard deviations are obtained with the high-frequency systems as long as the damping ratios are higher than approximately 0.1. For flight tasks that require accurate positioning of the aircraft, such as landing approaches, display configurations with fields of view in the range from  $\pm 15^\circ$  to  $\pm 30^\circ$  and distances in the range from 100 to 400 m would have to be considered.

For en route control tasks, accurate positioning of the aircraft is not required; but ease in finding the box, if it is not in the field of view, and keeping the box in view are more important. Wide fields of view and long distances to the box enhance these factors. Therefore, a field of view of  $\pm 45^\circ$  and a distance to the box from 1000 to 6000 m should be considered.

The total outer-loop displacement gains of the system are a function of aircraft velocity. That is, the effective outer-loop vertical and lateral gains are  $K_h V$  and  $K_y V$ . The velocity used in the present tests was 85 knots, which was the approach speed of the aircraft. For tasks undertaken at velocities other than 85 knots, it will be necessary to consider the effect of this change in velocity and adjust the distance to the box accordingly.

#### CONCLUDING REMARKS

A simulator study of the use of a pictorial aircraft-guidance display has been conducted. The simulator modeled a typical four-place, single-engine, high-wing aircraft. The pilot's task was to regulate aircraft positions and keep errors as small as possible. The display presents a drawing of a three-dimensional box that is located on the desired path and moves along that path ahead of the aircraft. The display can be implemented with an onboard digital computer, a cathode-ray-tube display device, and conventional aircraft navigation and attitude sensors. The purpose of the study was to examine the effect on the pilot-aircraft-display system response

of varying the field of view and distance to the box, both of which are design parameters of the display. Pilot ratings, system performance, and system-response characteristics were determined.

The pilots preferred the display configuration that used distances to the box of 368 m (1200 ft) and 915 m (3000 ft) and a field of view of  $\pm 30^\circ$ . Shorter distances resulted in higher system frequencies and longer distances resulted in lower system frequencies, both of which the pilots preferred less. Fields of view larger or smaller than  $\pm 30^\circ$  resulted in less system damping, which the pilots preferred less.

The best performance, both in the sense of quickness of error correction and lower standard deviations of lateral- and vertical-position errors, was obtained with a short distance to the box of 92 m (300 ft) and a field of view of  $\pm 15^\circ$ . With a narrower field of view of  $\pm 5^\circ$ , the system damping was so low that performance was adversely affected. Longer distances to the box resulted in lower system frequencies, slow system response, and large errors.

As is the case with other display concepts, compromises based on pilot preference, work load, and system performance must be made in selecting the parameters of the display. A thorough understanding of the effects of the design parameters of the display is, therefore, required. The results of this simulator study contribute toward the required understanding of the pictorial display for general aviation type aircraft.

Langley Research Center  
National Aeronautics and Space Administration  
Hampton, VA 23665  
November 2, 1983

## APPENDIX

### LINEARIZED PILOT-AIRCRAFT-DISPLAY EQUATIONS

The following linearized lateral and vertical sets of equations were used to determine the characteristics of the pilot-aircraft-display system:

For lateral response,

$$\ddot{\beta} = -0.229\beta + 0.0065r - 0.0162p + 0.225\phi - r$$

$$\ddot{p} = -6.95\beta + 1.10r - 4.82p - 8.53\delta_a$$

$$\ddot{r} = 2.85\beta - 0.725r - 0.436p + 0.216\delta_a$$

$$\dot{\phi} = p$$

$$\dot{\delta}_a = \delta'_a$$

$$\ddot{\delta}_a = -25\delta_a - 10\delta'_a + 25K_\phi\phi + 25K_\phi K_\psi\psi + 25K_\phi K_\psi K_y y$$

$$\dot{\psi} = \frac{g}{V} \phi$$

$$\ddot{y} = v\psi$$

For vertical response,

$$\ddot{\alpha} = -1.03\alpha + q$$

$$\ddot{q} = -1.21q - 2.82\alpha - 3.05\delta_e$$

$$\ddot{\theta} = q$$

$$\dot{\delta}_e = \delta'_e$$

$$\ddot{\delta}_e = -25\delta_e - 10\delta'_e + 25K_\theta\theta + 25K_\theta K_h h$$

$$\ddot{h} = v(\theta - \alpha)$$

#### REFERENCES

1. Adams, James J.; and Lallman, Frederick J.: Description and Preliminary Studies of a Computer Drawn Instrument Landing Approach Display. NASA TM-78771, 1978.
2. Adams, James J.: Simulator Study of Conventional General Aviation Instrument Displays in Path-Following Tasks With Emphasis on Pilot-Induced Oscillations. NASA TP-1776, 1980.
3. Adams, James J.: Simulator Study of a Pictorial Display for General Aviation Instrument Flight. NASA TP-1963, 1982.
4. Adams, James J.: Flight-Test Verification of a Pictorial Display for General Aviation Instrument Approach. NASA TM-83305, 1982.
5. Adams, James J.: Simulator Study of a Flight Director Display. NASA TM-84581, 1983.
6. Jacobson, Ira D.; and Joshi, Dinesh S.: Effects of Simulated Turbulence on Aircraft Handling Qualities. Rep. No. UVA/528066/ESS77/106 (Grant No. NGR 47-005-208(4)), Dep. Eng. Sci. & Syst., Univ. of Virginia, Mar. 1977. (Available as NASA CR-152621.)
7. Adams, James J.: Pilot-Model Measurements of Pilot Responses in Lateral-Directional Control Task. NASA TN D-8357, 1976.



TABLE I.- PILOT RANKING

Subject	Pilot ranking for configuration -													
	1	2	3	4	5	6	7	8	9	10	11	12	13	14
1	5	3.5	3.5 2	2	6	5.5	2.5 2	2		4 3.5	3 2	2.5	2.5	3
2	5	3	3 2	4	7	2	4 1	4	4	4	3 1	5 2	2	6
3	6.5	6	6 4	5	6.5	5.5	4	4	5.5	4 5	3 5	3	2.5	5
4	7	6	3	3	7	6	4 3	3	6	4 7	3 2.5		2.5	2
5	6	3	5 5	6	7	5	3 5 2	2	6	4	3 2	3	5	6
6	8	7	7 7 7	7 7	8	7	5 6 6.5	6	7	4 5	3 4	5 3	2.5	7
7	6	4	5 3.5	3.5	6	2.5	2 3.5	3.5	5	4 4	3 2	5 3	3	6

Configuration Number

Distance to box		Field of view -			
m	ft	$\pm 5^\circ$	$\pm 15^\circ$	$\pm 30^\circ$	$\pm 45^\circ$
92	300	1	2	3	4
184	600	5	6	7	8
368	1 200	9	10	11	12
915	3 000			13	
6100	20 000			14	

TABLE II.- RANK ORDERING OF CONFIGURATIONS BY EACH SUBJECT


Subject	Rank ordering of configuration													
	Best  Worst													
1	8	4	7	12	13	11	3	14	2	10	1	6	5	
2	11	13	6	3	7	2	12	10	9	8	4	1	14	5
3	13	12	7	8	11	10	14	3	4	6	9	2	1	5
4	14	13	11	8	4	3	7	10	6	2	9	1	5	
5	8	11	12	2	7	10	13	6	3	4	9	14	1	5
6	13	11	12	10	8	7	14	6	4	3	2	9	1	5
7	11	6	7	13	8	4	10	12	2	3	9	14	1	5

TABLE III.- LATERAL STANDARD DEVIATION

(a) All values are given in SI Units

Subject	Lateral standard deviation, m, for configuration -													
	1	2	3	4	5	6	7	8	9	10	11	12	13	14
1		7.22	3.38 5.24	6.10	8.81	7.24	12.43	4.25	12.69 9.32	12.34 20.62	9.18 8.33	7.95	16.56	48.31
2		5.68	5.99 4.36	6.45	3.75	6.36	5.82 6.28	7.95	7.54	6.93	6.37 8.00	11.08	13.72	45.33
3	3.83	8.15	11.6 4.65	9.0	13.3 6.23	6.55	6.40 5.09	9.70	7.53	14.1	8.70 5.17	12.3	15.3	15.1
4		3.42	6.60	4.64		4.31	6.37 8.98	15.38	11.55	20.08	10.65 7.72	10.10	25.10	50.64
5	3.52	3.78	3.58	7.75	6.51	2.63	7.18 5.89	5.24	5.01	5.89	4.31 6.70	6.57	10.26	16.08
6		5.35	10.75	8.07	7.67	6.64	3.28 7.43	10.84	7.71	4.96 9.25	4.68 7.00	8.53	10.22	21.56
7		6.84	9.88 6.45	7.40	5.73	8.43	8.67 5.37	11.95	7.36	8.42	5.79 11.20	8.66	12.00	11.85
Average ...		5.78	6.59	7.06	7.43	6.02	6.86	9.33	8.59	11.40	7.41	9.31	14.74	29.84

TABLE III.- Concluded

(b) All values are given in U.S. Customary Units

Subject	Lateral standard deviation, ft, for configuration -													
	1	2	3	4	5	6	7	8	9	10	11	12	13	14
1		23.7	11.1 17.2	20.0	28.9	23.8	40.8	13.9	41.6 30.6	40.5 67.6	30.1 27.3	26.1	54.3	158.5
2		18.6	19.7 14.3	21.1	12.3	20.9	19.1 20.6	26.1	24.7	22.7	20.9 26.2	36.3	45.0	148.7
3	12.6	26.7	38.1 15.3	29.5	43.6 20.4	21.5	21.0 16.7	31.8	24.7	46.3	28.5 17.0	40.4	50.2	49.5
4		11.2	21.7	15.2		14.1	20.9 29.5	50.5	37.9	65.9	34.9 25.3	33.1	82.4	166.1
5	11.5	12.4	11.7	25.4	21.3	8.6	23.6 19.3	17.2	16.4	19.3	14.1 22.0	21.6	33.7	52.8
6		17.6	35.3	26.4	25.2	21.8	10.8 24.4	35.6	25.3	16.3 30.3	15.4 23.0	28.0	33.5	70.7
7		22.4	32.4 21.1	24.2	18.8	27.6	28.4 17.6	39.2	24.1	27.6	19.0 36.7	28.4	39.4	38.9
Average ...		18.9	21.6	23.2	24.4	19.8	22.5	30.6	28.2	37.4	24.3	30.5	48.4	97.9

TABLE IV.- LATERAL MEANS

(a) All values are given in SI Units

Subject	Lateral means, m, for configuration -													
	1	2	3	4	5	6	7	8	9	10	11	12	13	14
1		4.40	2.24 4.99	4.14	8.00	6.72	-1.09	1.86	16.55 19.99	15.76 4.74	6.97 10.79	5.20	6.32	56.24
2		3.44	4.32 2.81	1.68	6.99	6.66	3.37 5.07	4.42	10.20	9.66	7.48 9.50	5.47	33.20	87.50
3	1.81	3.08	3.92 2.86	0.03	2.26 6.80	4.26	1.65 4.05	3.52	3.52	-1.91	4.00 3.26	3.70	2.17	-6.86
4		3.20	5.04	4.33		6.28	1.89 9.95	9.81	21.50	17.61	12.42 9.03	9.98	19.43	65.50
5	2.84	2.92	1.73	1.95	3.69	2.94	2.24 2.06	1.01	11.98	6.93	7.35 3.74	7.69	10.01	19.89
6		4.47	2.36	1.39	8.28	4.56	0.48 1.80	3.75	6.69	4.47 12.03	1.35 2.12	8.53	2.30	1.41
7		3.77	0.37 1.32	0.86	3.03	4.54	2.76 .57	4.60	9.46	1.69	4.75 5.94	0.22	5.37	0.90
Average ...		3.61	2.91	2.05	5.58	5.14	2.68	4.14	12.48	7.92	6.33	5.82	11.26	32.08

TABLE IV.- Concluded

(b) All values are given in U.S. Customary Units

Subject	Lateral means, ft, for configuration -													
	1	2	3	4	5	6	7	8	9	10	11	12	13	14
1		14.4	7.3 16.4	13.6	26.2	22.0	-3.6	6.1	54.3 65.6	51.7 15.6	22.9 35.4	17.1	20.7	184.5
2		11.3	14.2 9.2	5.5	22.9	21.8	11.0 16.6	14.5	33.5	31.7	24.5 31.2	17.9	108.9	287.1
3	5.9	10.1	12.9 9.4	0.1	7.4 22.3	14.0	5.4 13.3	11.5	11.5	-6.3	13.1 10.7	12.1	7.1	-22.5
4		10.5	16.5	14.2		20.6	6.2 32.6	32.2	70.5	57.8	40.8 29.6	32.7	63.7	214.9
5	9.3	9.6	5.7	6.4	12.1	9.6	7.3 6.7	3.3	39.3	22.7	24.1 12.3	25.2	32.8	65.3
6		14.7	7.7	4.6	27.2	15.0	1.6 5.9	12.3	21.9	14.7 39.5	4.4 7.0	30.0	7.5	4.6
7		12.4	2.8 4.3	2.9	9.9	14.9	9.1 1.9	15.1	31.0	5.5	15.6 19.5	0.7	17.6	2.9
Average ...		11.9	9.5	6.7	18.3	16.9	8.8	13.6	40.9	26.0	20.8	19.1	36.9	105.3

TABLE V.- VERTICAL STANDARD DEVIATION

(a) All values are given in SI Units

Subject	Vertical standard deviations, m, for configuration -													
	1	2	3	4	5	6	7	8	9	10	11	12	13	14
1		2.08	2.26 2.14	2.89	5.57	5.16	5.08	5.93	11.98 7.06	13.86 8.82	7.31 6.39	15.16	7.60	28.86
2		2.09	2.10 1.50	2.41	3.81	5.00	3.66 2.07	2.71	4.89	4.36	5.14 5.29	3.93	6.41	11.90
3	2.21	3.09	4.86 3.66	4.73	5.60 4.70	2.94	4.40 3.41	6.20	4.61	11.10	11.10 5.65	8.80	12.7	5.00
4		2.65	3.84	4.41		5.48	5.89 6.66	11.30	5.76	13.56	8.53 3.42	4.82	8.84	8.02
5	1.85	2.16	2.70	2.61	3.33	1.97	3.79 2.75	3.11	5.14	5.45	3.92 4.55	4.73	10.42	6.12
6		2.21	4.05	3.24	5.47	2.97	3.65 3.88	4.71	7.40	3.86 11.55	4.18 5.06	4.58	6.81	4.53
7		2.64	4.38 3.10	3.07	6.03	3.13	4.97 2.64	4.62	6.50	8.77	8.05 5.39	11.14	8.09	16.50
Average ...		2.42	3.14	3.34	4.93	3.80	4.06	5.51	6.67	9.04	5.99	7.66	8.69	11.56

TABLE V.- Concluded

(b) All values are given in U.S. Customary Units

Subject	Vertical standard deviation, ft, for configuration -													
	1	2	3	4	5	6	7	8	9	10	11	12	13	14
1		6.8	7.4 7.0	9.5	18.2	16.9	16.7	19.4	39.3 23.2	45.4 28.9	24.0 21.0	49.7	24.9	94.7
2		6.8	6.8 4.9	7.9	12.5	16.4	12.0 6.8	8.9	16.1	14.3	16.9 17.3	12.9	21.0	39.0
3	7.3	10.1	15.9 12.0	15.5	18.4 15.4	9.6	14.4 11.2	20.3	15.1	36.4	36.4 18.5	28.9	41.7	16.4
4		8.7	12.6	14.5		18.0	19.3 21.8	37.1	18.9	44.5	28.0 11.2	15.8	29.0	26.3
5	6.1	7.1	8.8	8.6	10.9	6.5	12.4 9.0	10.2	16.9	17.9	12.9 14.9	15.5	34.2	20.1
6		7.3	13.3	10.6	17.9	9.7	12.0 12.7	15.4	24.3	12.7 37.9	13.7 16.6	15.0	22.3	14.8
7		8.7	14.4 10.2	10.1	19.8	10.3	16.3 8.7	15.2	21.3	28.8	26.4 17.7	36.6	26.5	54.1
Average ...		7.9	10.3	11.0	16.2	12.5	13.3	18.1	21.9	29.7	19.6	25.1	28.5	37.9



TABLE VI.- VERTICAL MEANS

(a) All values are given in SI Units

Subject	Vertical means, m, for configuration -													
	1	2	3	4	5	6	7	8	9	10	11	12	13	14
1		0.88	0.10 0	1.26	-1.40	-1.07	1.74	1.36	5.33 2.89	-5.88 1.19	1.49 -2.95	-0.41	2.24	-14.15
2		-0.45	0.06 .49	1.04	-0.90	0.62	-0.56 1.71	2.43	7.69	-3.74	0.41 -.88	-6.48	-0.31	-0.70
3	0.67	2.40	1.53 -.03	-2.6	-2.74 -.04	-0.05	-1.97 -1.80	4.3	0.73	-4.63	2.98 -2.40	-4.30	2.96	8.40
4		0.98	-0.86	1.31		0.48	1.44 1.58	-3.44	4.13	-0.44	2.20 4.50	11.37	-0.66	-0.75
5	0.27	0.27	0.89	-0.57	-1.07	1.91	-0.08 .71	-1.59	-4.92	-5.71	-0.44 1.35	4.04	1.52	5.16
6		-2.53	-1.51	-0.10	-3.66	0.65	-0.08 -.48	-2.55	1.10	-3.79 -11.56	-2.93 3.88	-3.74	-6.52	-2.30
7		0.63	1.35 1.07	0.57	0.96	1.22	2.18 .83	1.0	1.6	-2.73	2.92 4.92	4.62	4.56	21.41
Average ...		0.31	0.28	0.13	-1.26	0.54	0.40	0.22	2.32	-4.14	1.07	0.73	0.54	2.44

TABLE VI.- Concluded

(b) All values are given in U.S. Customary Units

Subject	Vertical means, ft, for configuration -													
	1	2	3	4	5	6	7	8	9	10	11	12	13	14
1		2.9	0.3 0	4.1	-4.6	-3.5	5.7	4.5	17.5 9.5	-19.3 3.9	4.9 -9.7	-1.3	7.3	-46.4
2		-1.5	0.2 1.6	3.4	-2.9	2.0	-1.8 5.6	8.0	25.2	-12.3	1.3 -2.9	-21.3	-1.0	-2.3
3	2.2	7.9	5.0 .1	-8.5	-9.0 -.1	-0.1	-6.5 -5.9	14.1	2.4	-15.2	9.8 -7.9	-14.1	9.7	27.6
4		3.2	-2.8	4.3		1.6	8.5 5.2	-11.3	13.6	-1.4	7.2 14.8	37.3	-2.1	-2.5
5	0.9	0.9	2.9	-1.8	-3.5	6.2	-0.3 2.3	-5.2	-16.1	-18.7	-1.4 4.4	13.2	5.0	16.9
6		-8.3	-4.6	-0.3	-12.0	2.1	-0.3 -1.6	-8.4	3.6	-12.4 -37.9	-9.6 12.7	-12.2	-21.3	-7.5
7		2.0	4.4 3.5	1.9	3.1	-4.0	7.2 2.7	3.3	5.2	-8.9	9.6 16.1	15.1	14.9	70.2
Average ...		1.0	0.9	0.4	-4.1	1.8	1.3	0.7	7.6	-13.6	3.5	2.4	1.8	8.0

TABLE VII.- RANK ORDERING OF STANDARD DEVIATION AND MEANS

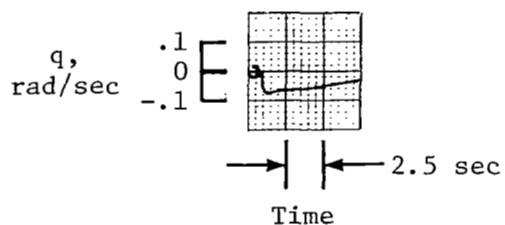
(a) All values are given in SI Units

Lateral standard deviation		Vertical standard deviation		Lateral means		Vertical means	
Configuration	Average, m	Configuration	Average, m	Configuration	Average, m	Configuration	Average, m
2	5.78	2	2.42	4	2.05	4	0.13
6	6.02	3	3.14	7	2.68	8	.22
3	6.59	4	3.34	3	2.91	3	.28
7	6.86	6	3.80	2	3.61	2	.31
4	7.06	7	4.06	8	4.14	7	.40
11	7.41	5	4.93	6	5.14	6	.54
5	7.43	8	5.51	5	5.58	13	.54
9	8.59	11	5.99	12	5.82	12	.73
12	9.31	9	6.67	11	6.33	11	1.07
8	9.33	12	7.66	10	7.92	5	-1.26
10	11.40	13	8.69	13	11.26	9	2.32
13	14.74	10	9.04	9	12.48	14	2.44
14	29.84	14	11.56	14	32.08	10	-4.14
1		1		1		1	

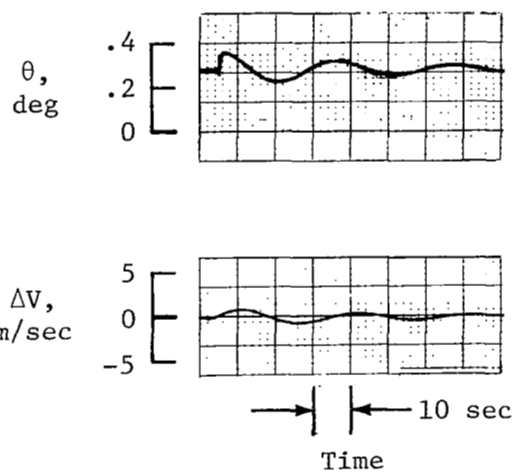
TABLE VII.- Concluded

(b) All values are given in U.S. Customary Units

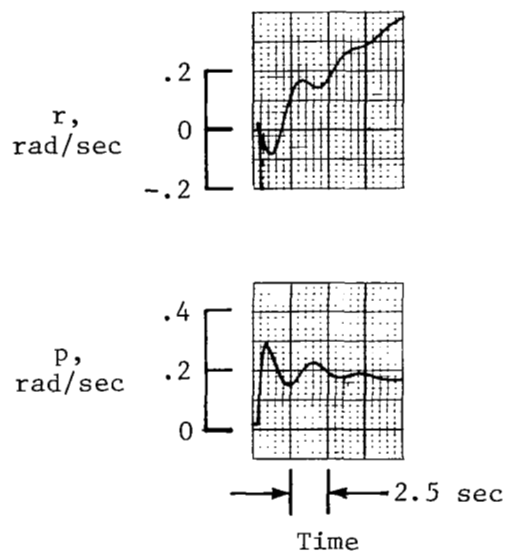
Lateral standard deviation		Vertical standard deviation		Lateral means		Vertical means	
Configuration	Average, ft	Configuration	Average, ft	Configuration	Average, ft	Configuration	Average, ft
2	18.9	2	7.9	4	6.7	4	0.4
6	19.8	3	10.3	7	8.8	8	.7
3	21.6	4	11.0	3	9.5	3	.9
7	22.5	6	12.5	2	11.9	2	1.0
4	23.2	7	13.3	8	13.6	7	1.3
11	24.3	5	16.2	6	16.9	6	1.8
5	24.4	8	18.1	5	18.3	13	1.8
9	28.2	11	19.6	12	19.1	12	2.4
12	30.5	9	21.9	11	20.8	11	3.5
8	30.6	12	25.1	10	26.0	5	-4.1
10	37.4	13	28.5	13	36.9	9	7.6
13	48.4	10	29.7	9	40.9	14	8.0
14	97.9	14	37.9	14	105.3	10	-13.6
1		1		1		1	



(a) Short-period response to 0.02-rad elevator step.

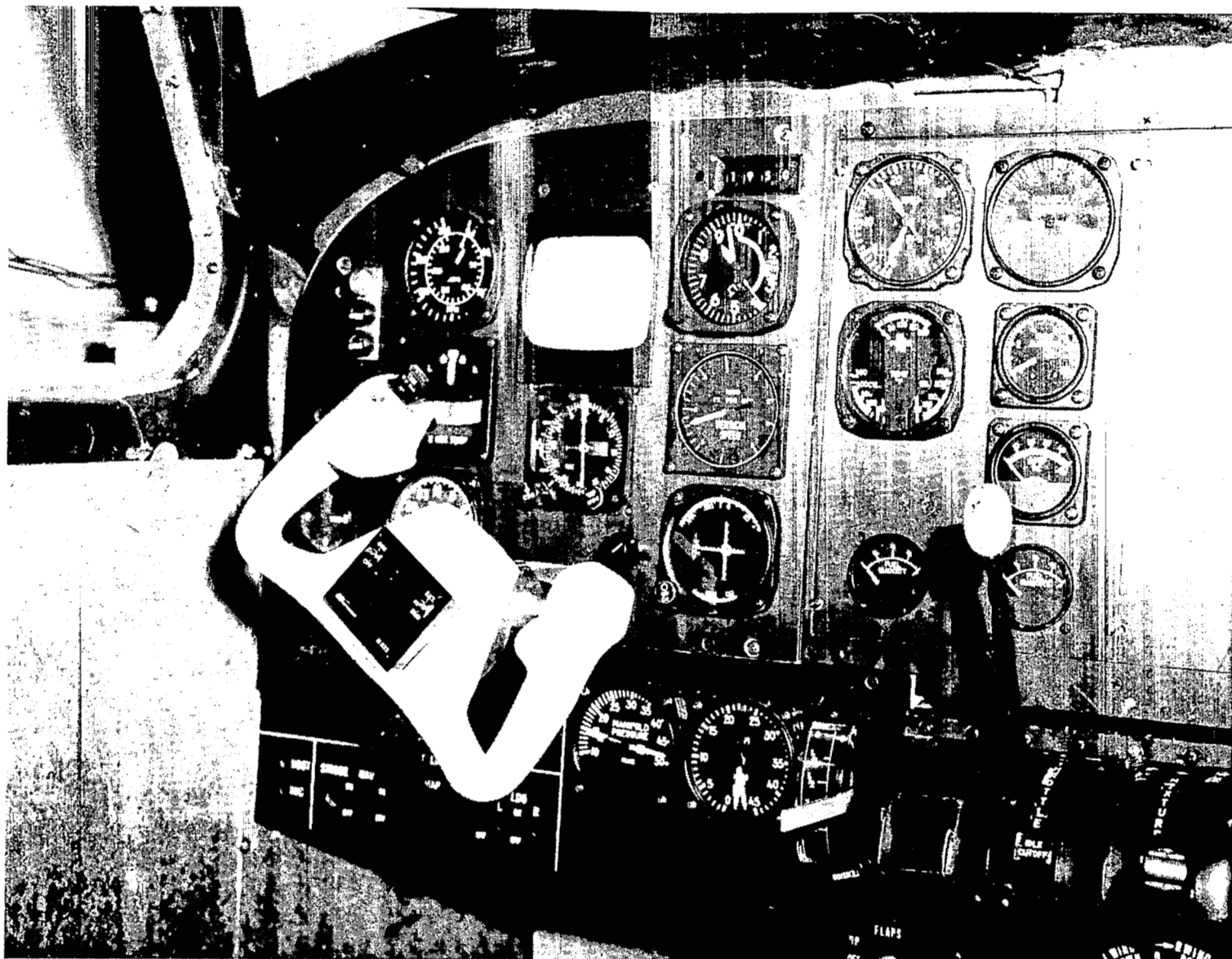


(b) Phugoid response to initial out-of-trim  $\alpha$ .



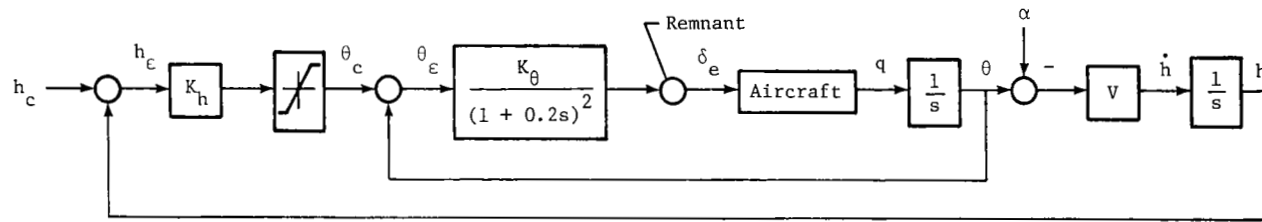
(c) Lateral response to 0.068-rad aileron step.

Figure 1.- Aircraft-response characteristics.

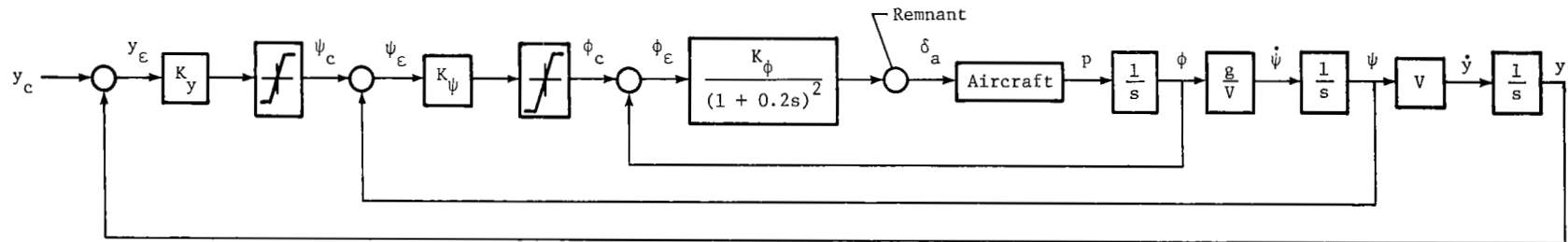


L-80-10,913

Figure 2.- Instrument panel of simulator.



(a) Longitudinal system.



(b) Lateral system.

Figure 3.- Block diagram of pilot-aircraft-display system.

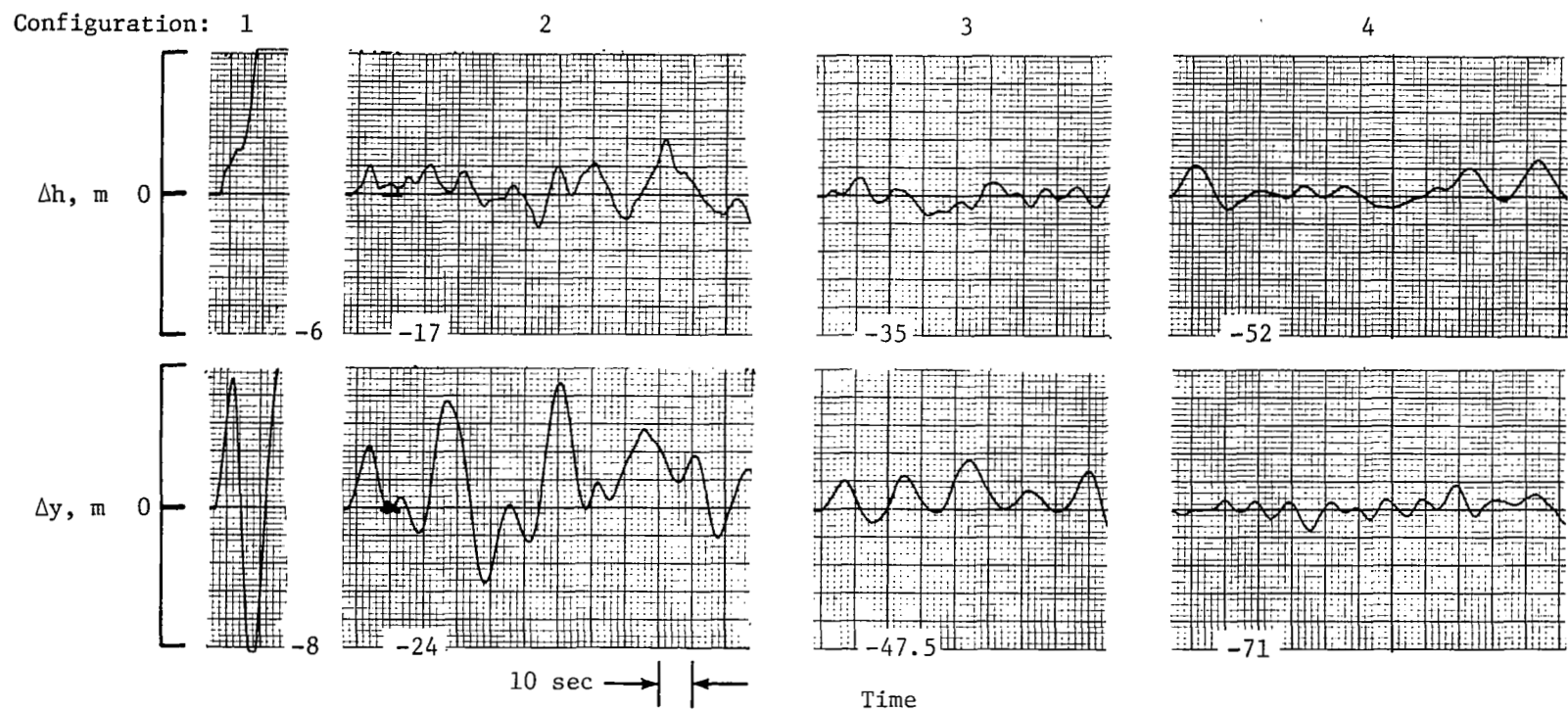


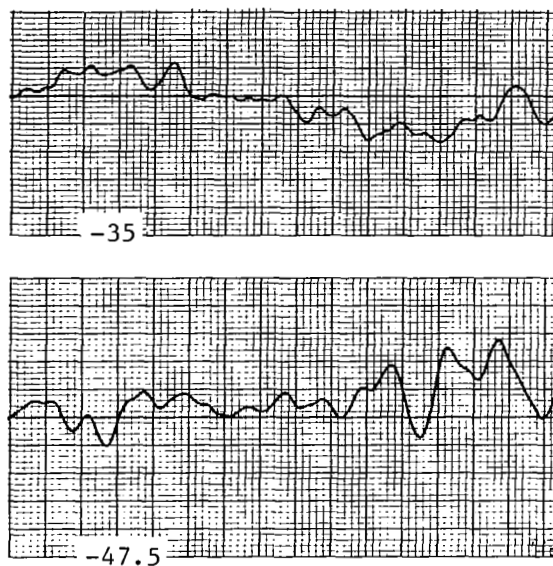
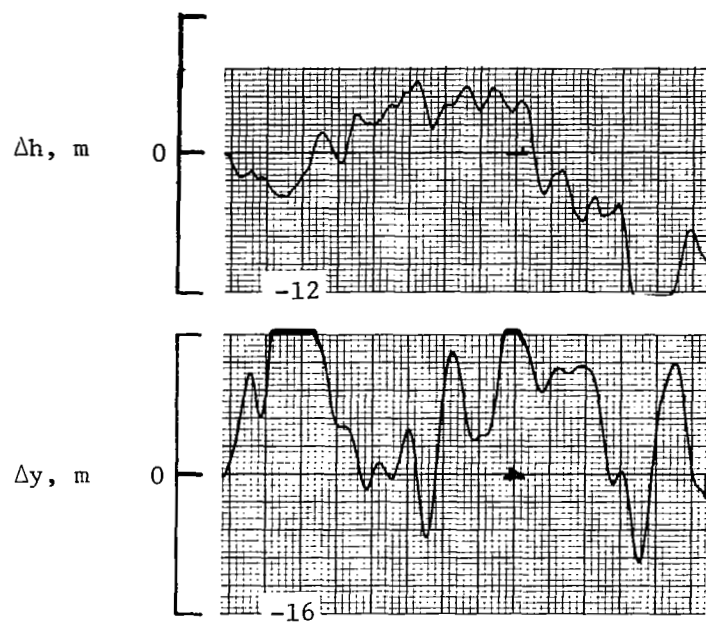
Figure 4.- System responses in presence of crosswind and gusts obtained with subject 1. Recording sensitivity changes with each configuration.



Configuration:

5

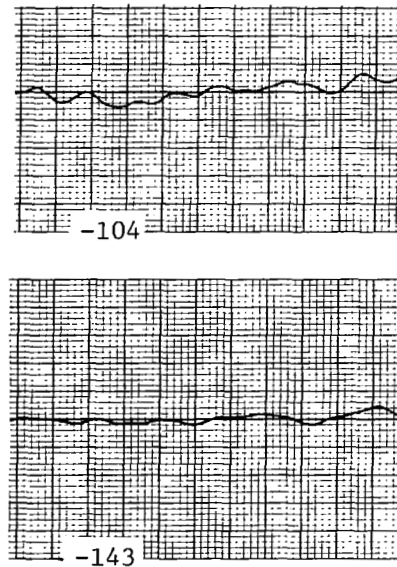
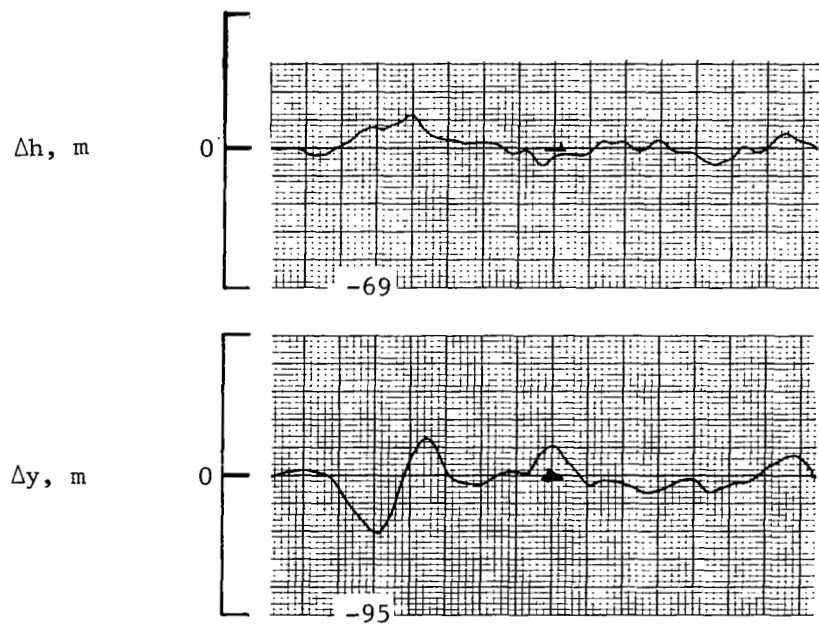
6



Configuration:

7

8



→ | | ← 10 sec

Time

Figure 4.- Continued.

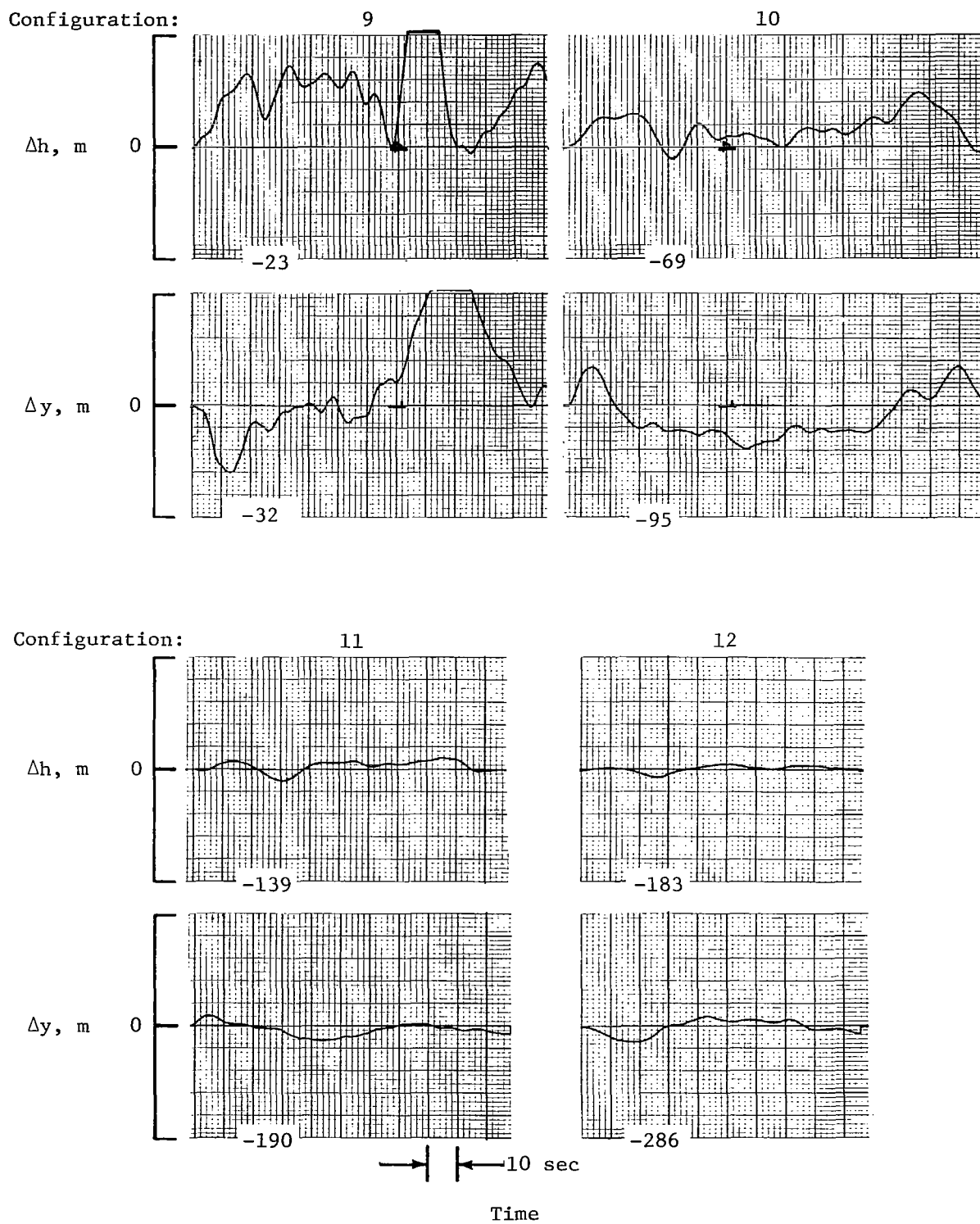


Figure 4.- Concluded.

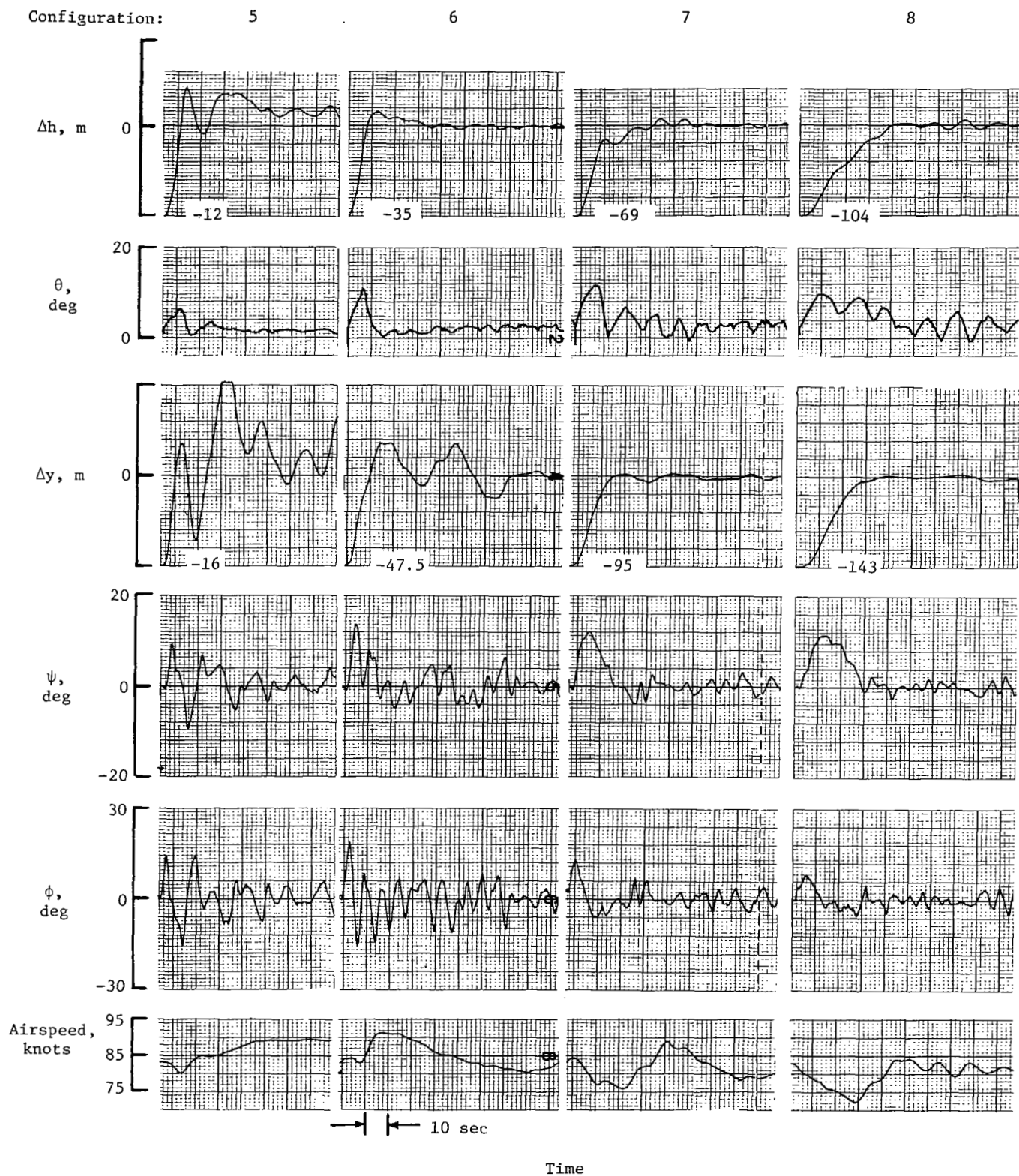


Figure 5.- System responses to initial error obtained with subject 1. Recording sensitivity changes with each configuration.

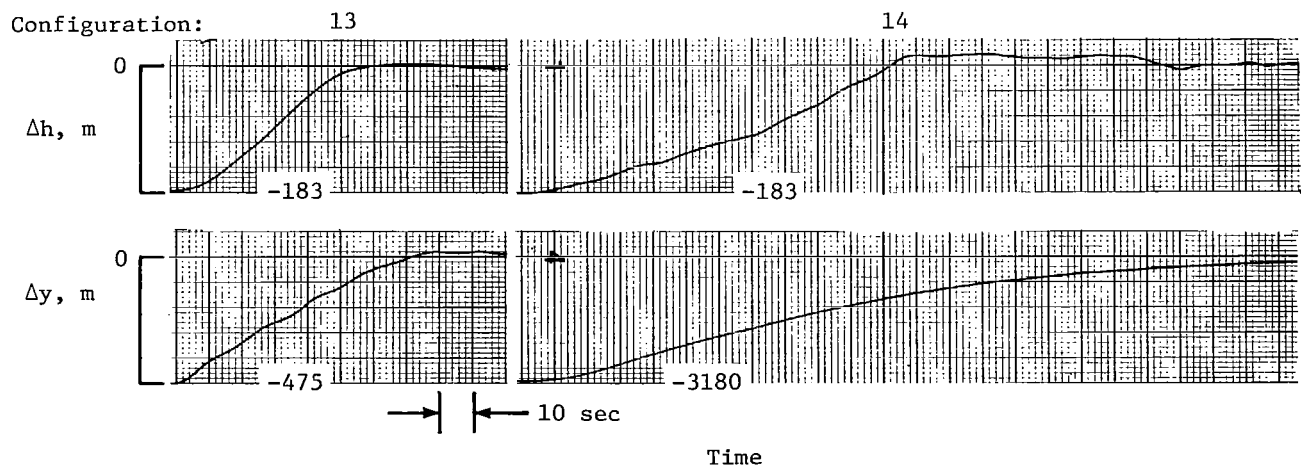
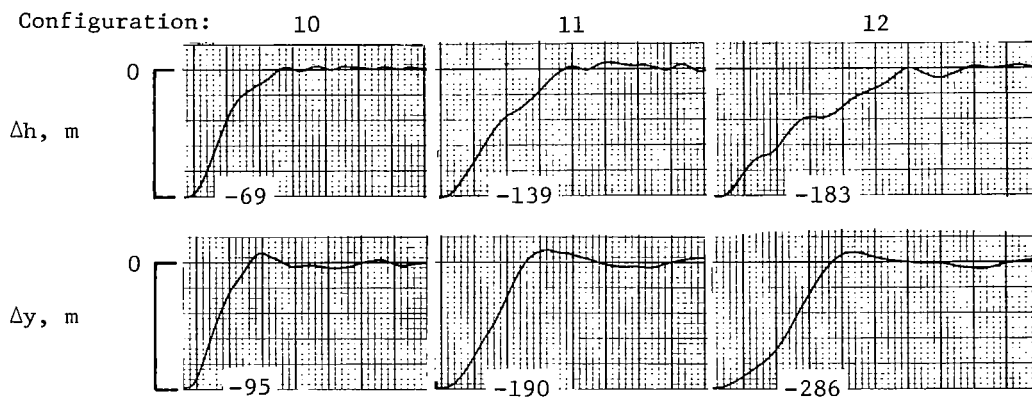
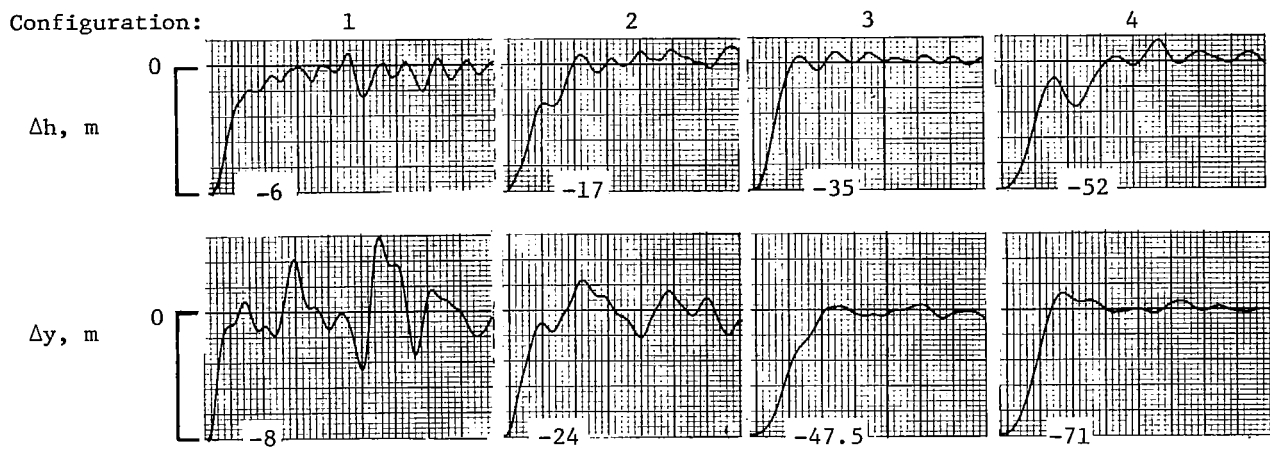


Figure 5.- Concluded.

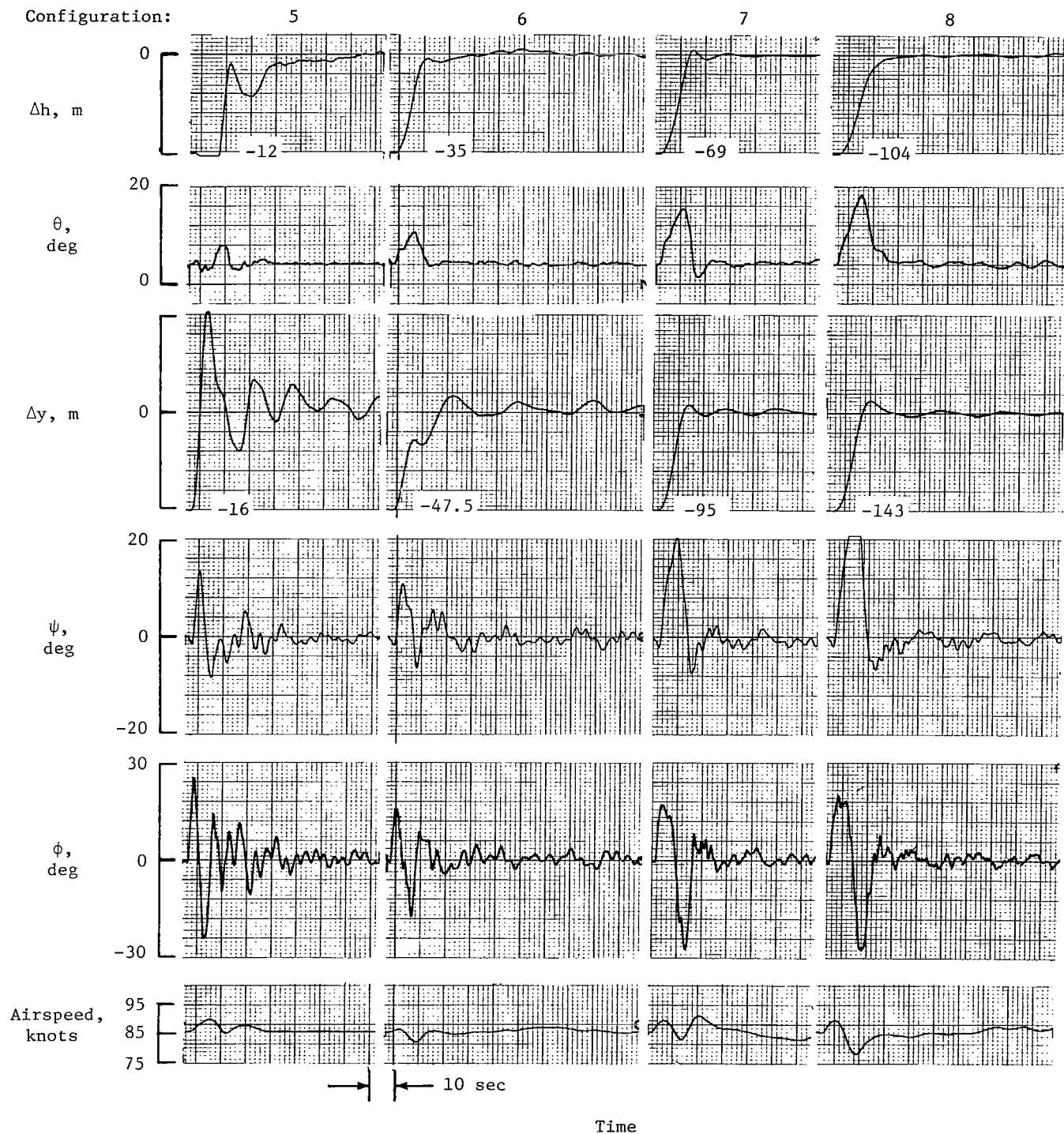
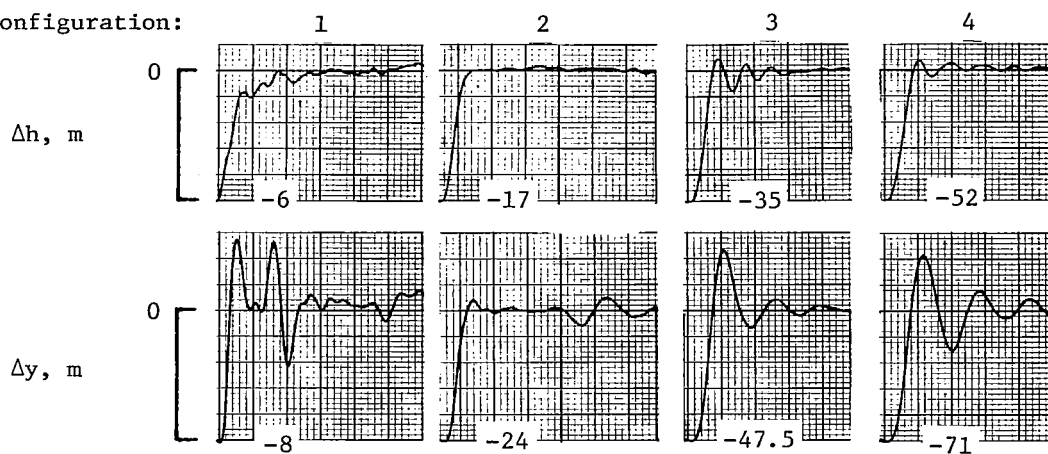
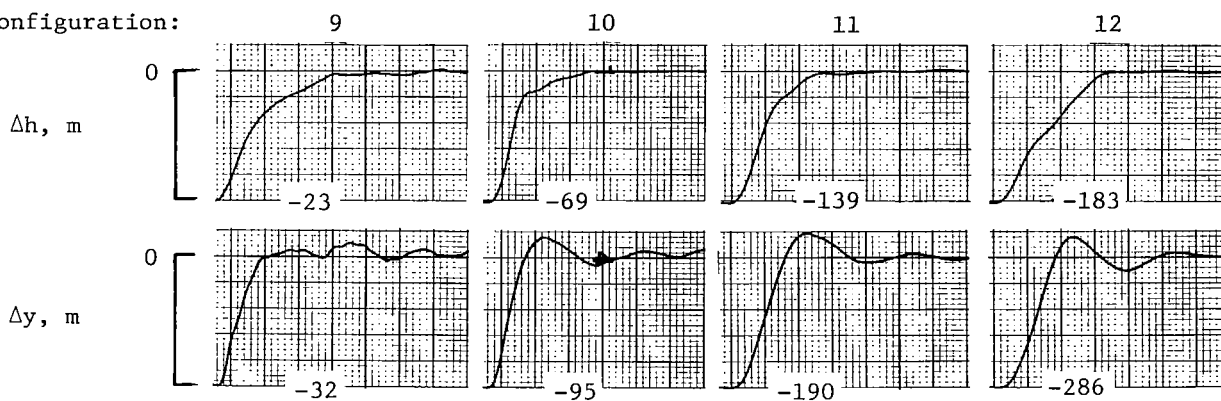


Figure 6.- System responses to initial error obtained with subject 5. Recording sensitivity changes with each configuration.

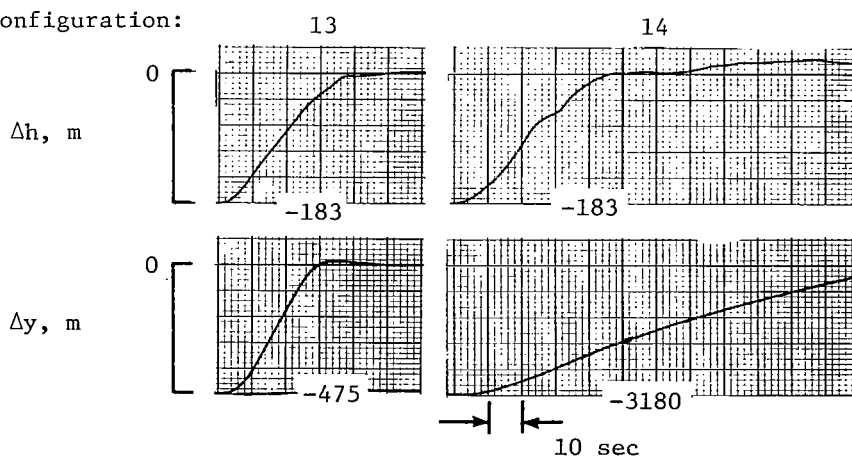
Configuration:



Configuration:



Configuration:



Time

Figure 6.- Concluded.

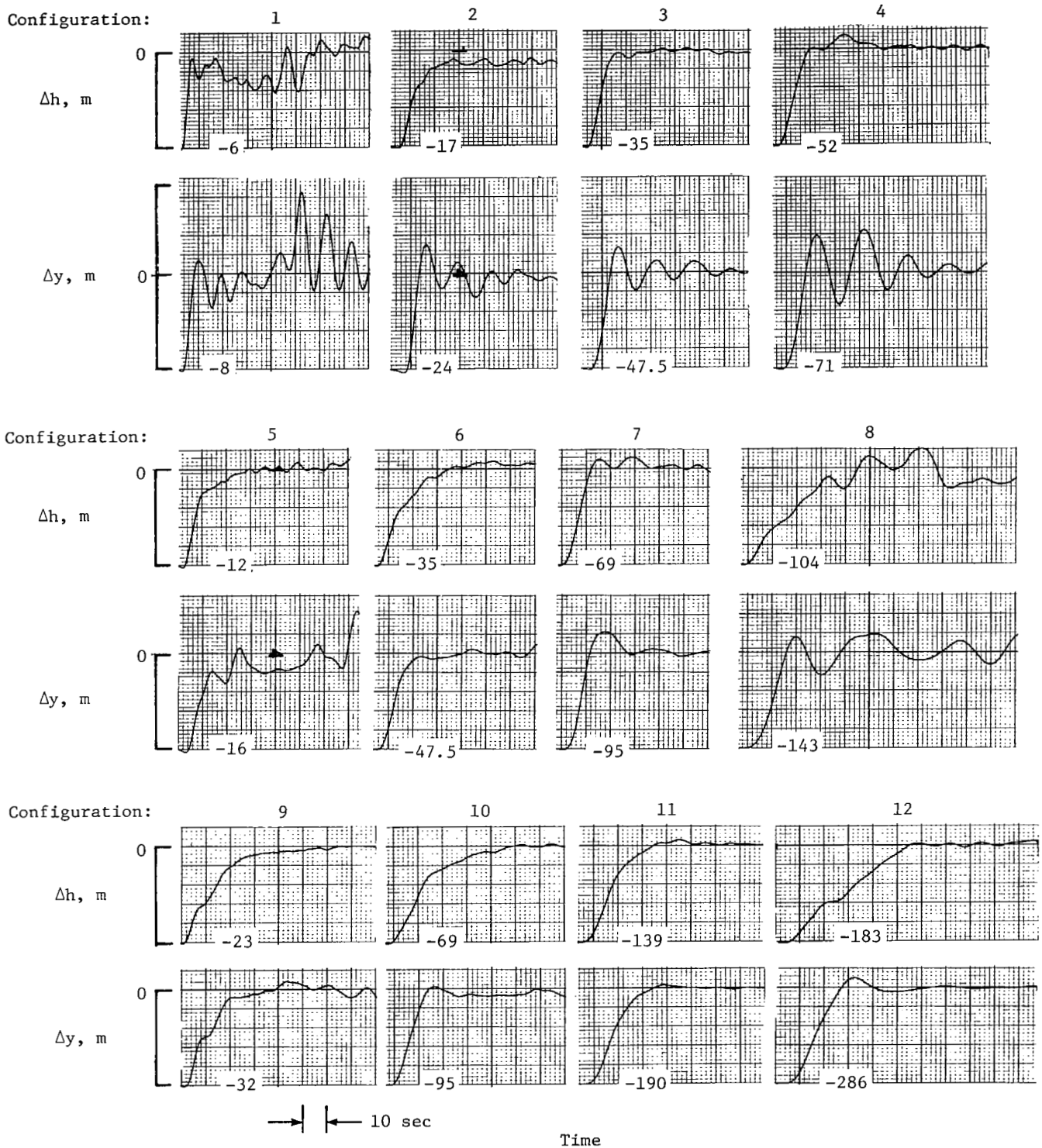


Figure 7.- System responses to initial errors obtained with subject 2. Recording sensitivity changes with each configuration.



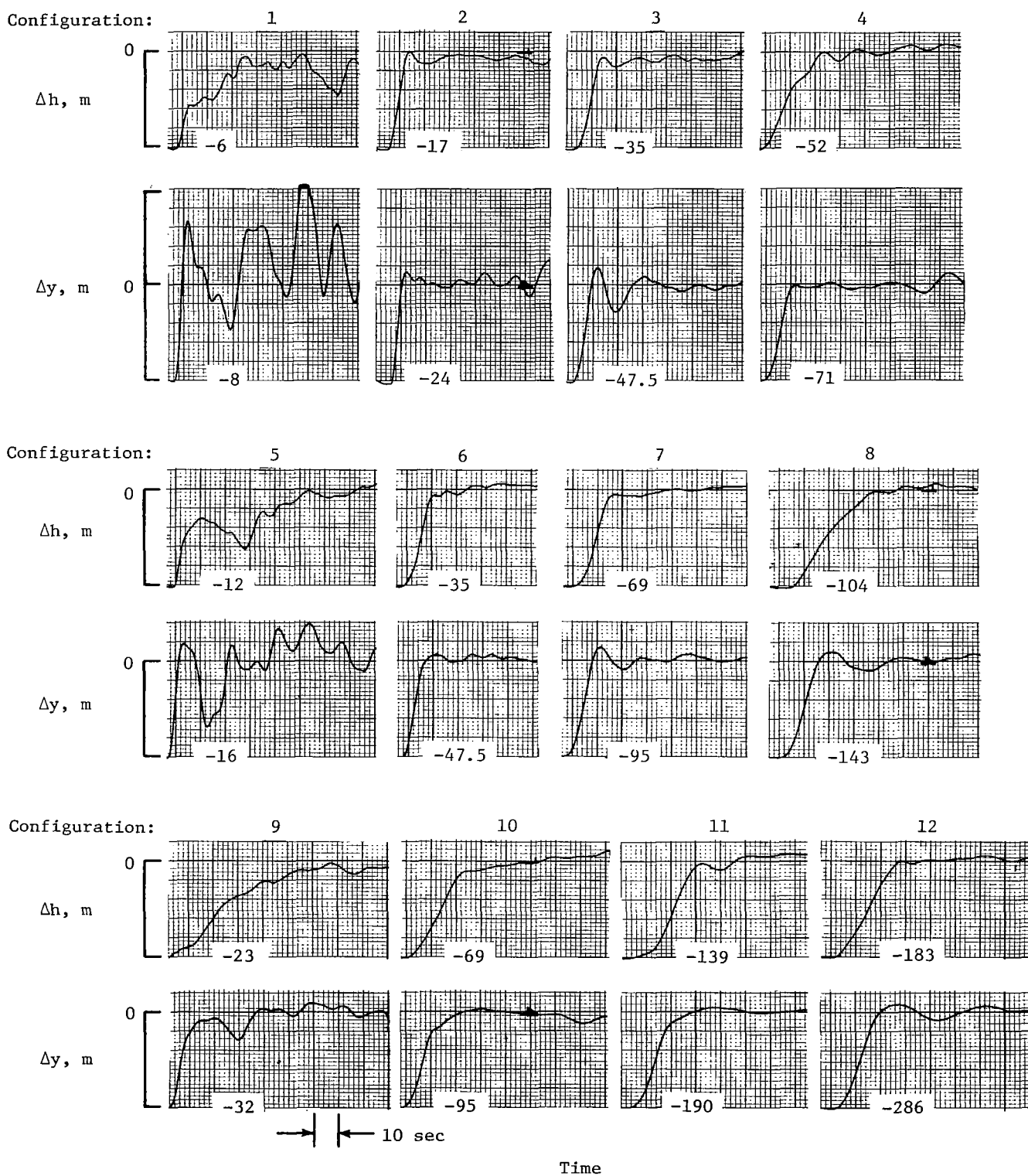


Figure 8.- System responses to initial errors obtained with subject 3. Recording sensitivity changes with each configuration.



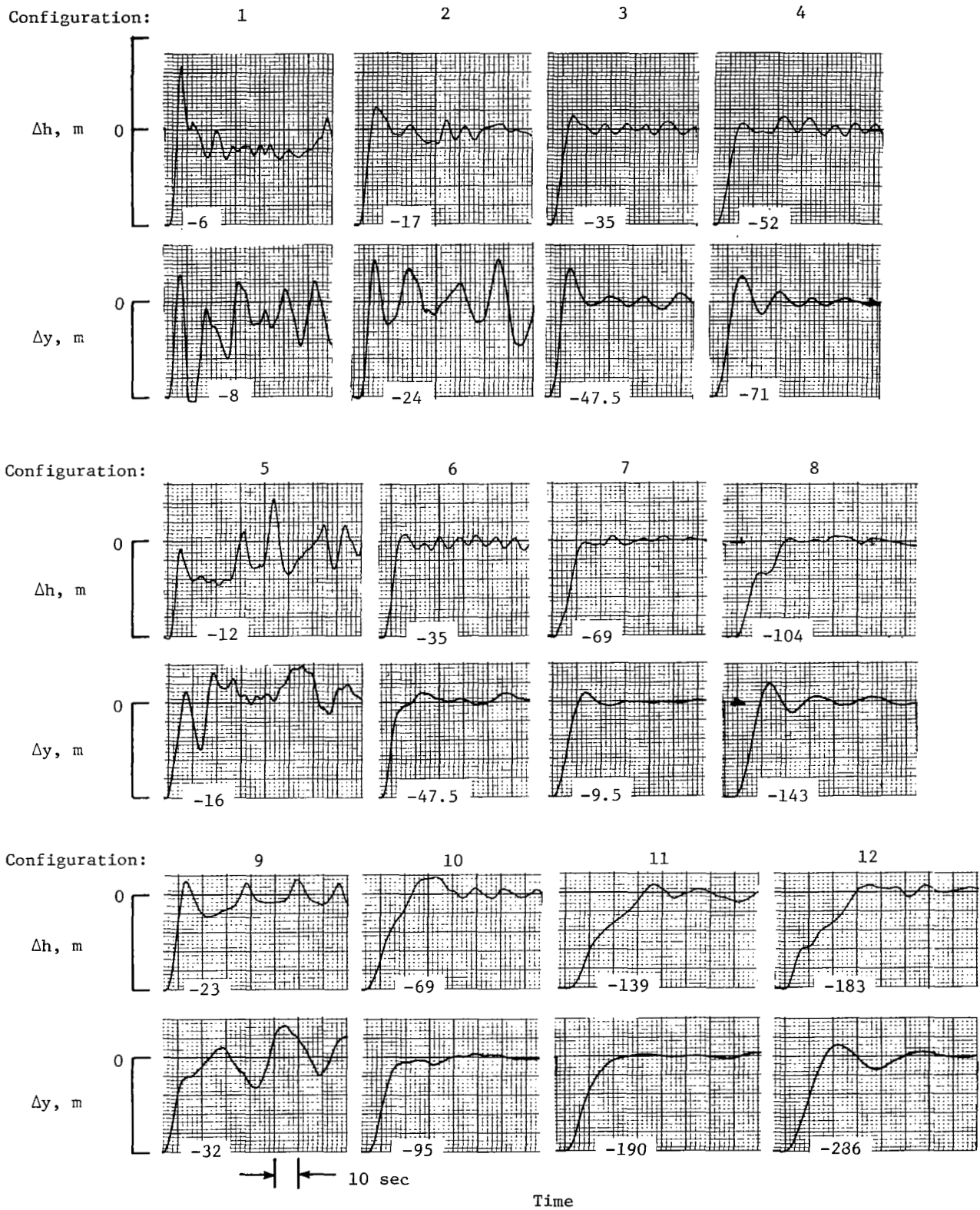
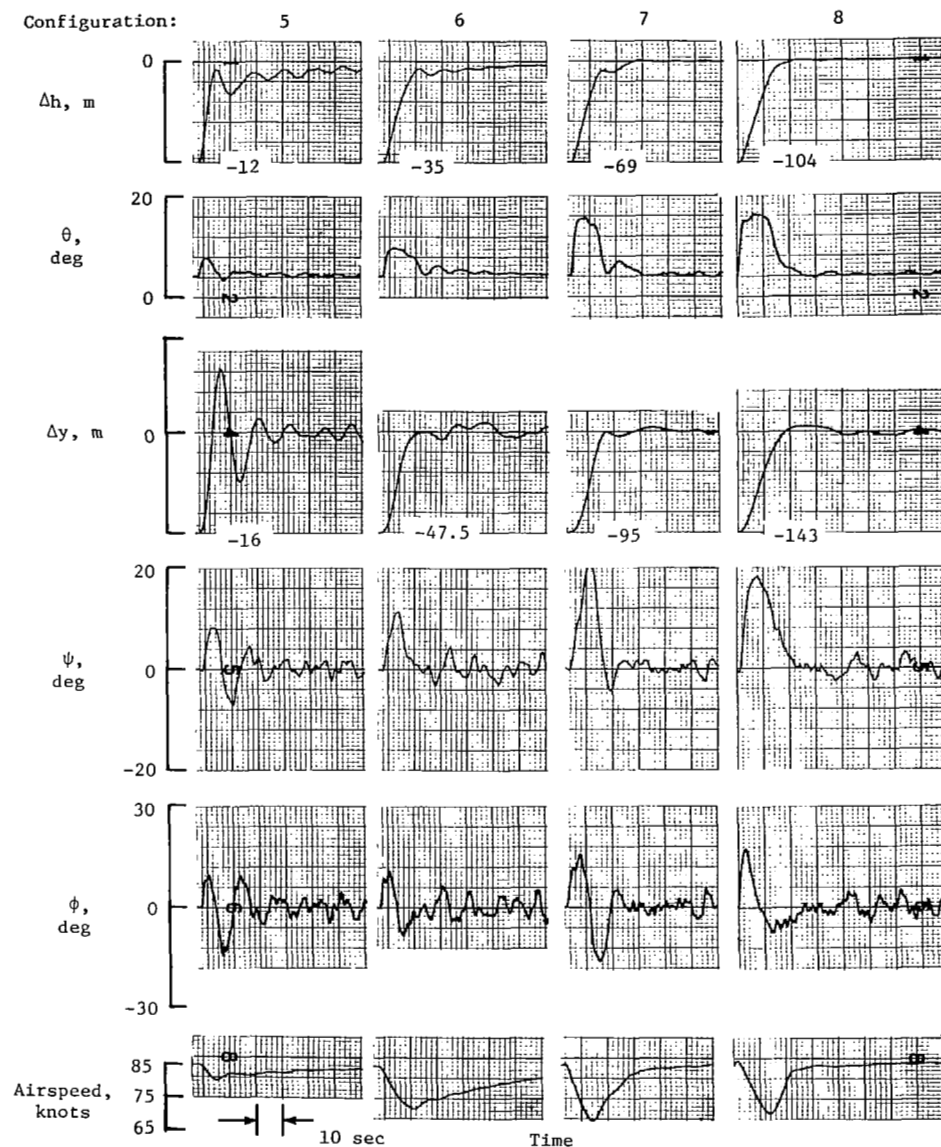
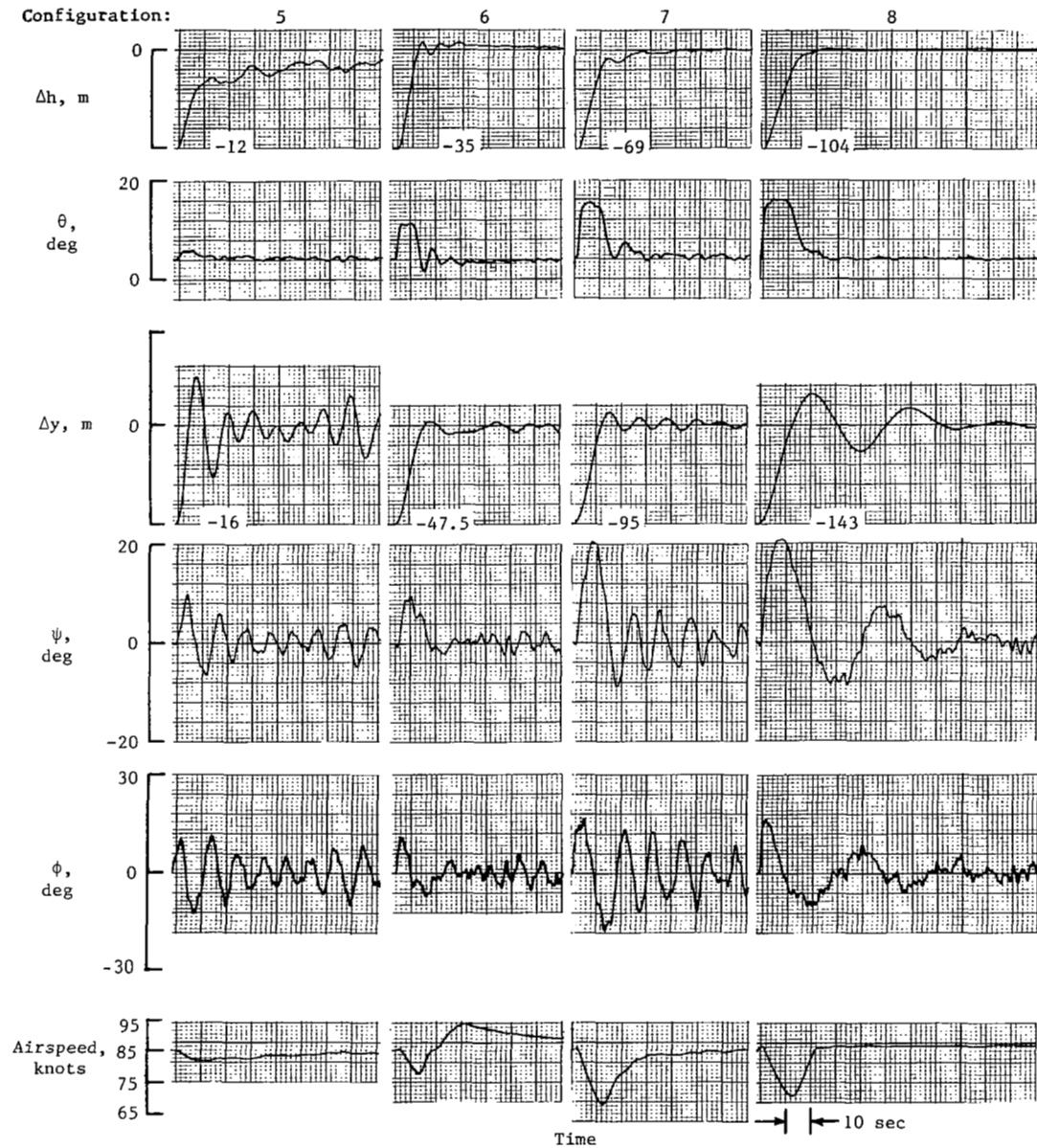


Figure 9.- System responses to initial errors obtained with subject 7. Recording sensitivity changes with each configuration.



Quantity	Responses from configuration -			
	5	6	7	8
$K_h$ , rad/m--	0.0097	0.0196	0.0097	0.0065
$K_\theta$ -----	-0.2	-0.4	-0.4	-0.2
$\theta_{c,L}$ , deg --	3.5	7	12	11.5
$K_y$ , rad/m--	0.0082	0.0033	0.0047	0.0033
$K_\psi$ -----	1.5	1.5	2	0.8
$K_\phi$ -----	-0.5	-0.5	-0.5	-0.5
$\psi_{c,L}$ , deg --			17	29
$\phi_{c,L}$ , deg --				

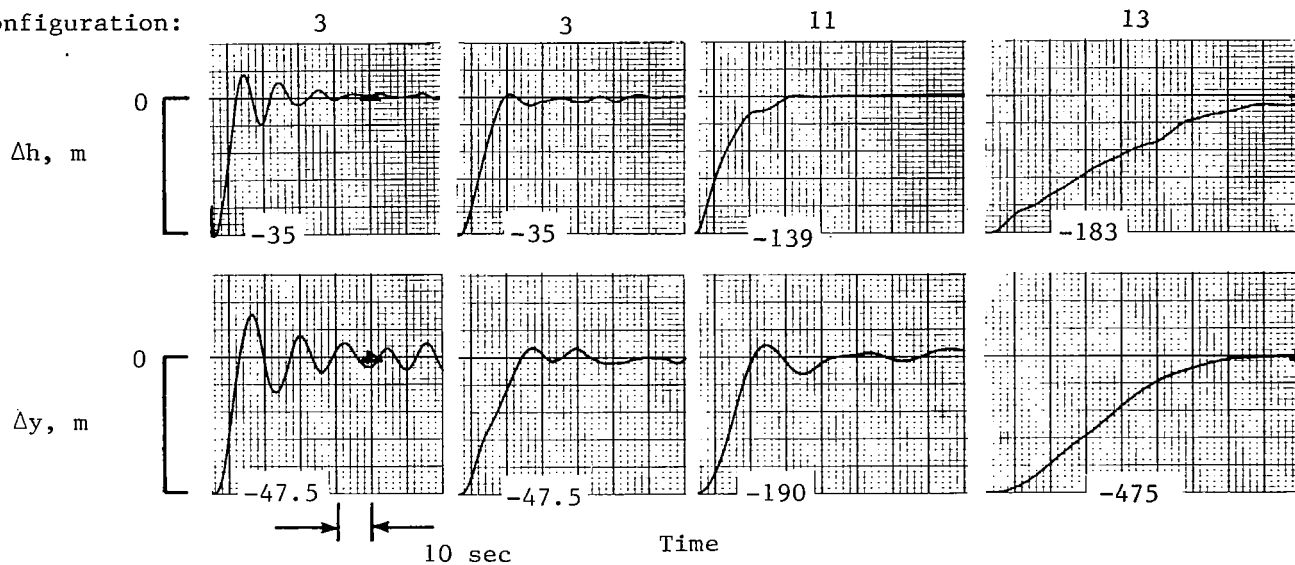
Figure 10.- System responses to initial errors obtained with pilot model. Recording sensitivity changes with each configuration.



Quantity	Responses from configuration -			
	5	6	7	8
$K_h$ , rad/m --	0.0097	0.0196	0.0097	0.0066
$K_\theta$ -----	-0.4	-0.6	-0.4	-0.2
$\theta_{c,L}$ , deg --		7	12	11
$K_y$ , rad/m --	-0.0082	0.0033	0.0066	0.0049
$K_\psi$ -----	2	1.5	2	0.5
$K_\phi$ -----	-0.5	-0.5	-0.5	-0.5
$\psi_{c,L}$ , deg --			17	29
$\phi_{c,L}$ , deg --			14	

Figure 10.- Continued.

Configuration:



Quantity	Responses from configuration -			
	3	3	11	13
$K_h, \text{rad/m} --$	0.0164	0.0164	0.0098	0.0098
$K_\theta -----$	-0.32	-0.24	-0.4	-0.32
$\theta_{c,L}, \text{deg} --$	11.5	5.7	19	4.3
$K_y, \text{rad/m} --$	0.0115	0.0082	0.0049	0.00164
$K_\psi -----$	1.5	1.5	1	1
$K_\phi -----$	-0.70	-0.70	-0.40	-0.40
$\psi_{c,L}, \text{deg} --$	12	4.3	43	14.3
$\phi_{c,L}, \text{deg} --$		5.7	17	5.7

Figure 10.- Concluded.

1. Report No. NASA TP-2122		2. Government Accession No.		3. Recipient's Catalog No.	
4. Title and Subtitle SIMULATOR STUDY OF PILOT-AIRCRAFT-DISPLAY SYSTEM RESPONSE OBTAINED WITH A THREE-DIMENSIONAL-BOX PICTORIAL DISPLAY				5. Report Date December 1983	
				6. Performing Organization Code 505-35-23-30	
7. Author(s) James J. Adams				8. Performing Organization Report No. L-15632	
				10. Work Unit No.	
9. Performing Organization Name and Address  NASA Langley Research Center Hampton, VA 23665				11. Contract or Grant No.	
				13. Type of Report and Period Covered Technical Paper	
12. Sponsoring Agency Name and Address  National Aeronautics and Space Administration Washington, DC 20546				14. Sponsoring Agency Code	
15. Supplementary Notes					
16. Abstract  This study examines the effect of varying the two important display parameters of a pictorial display on pilot opinion, performance, and pilot-aircraft-display system servomechanism response. The display presents a picture of a three-dimensional box that moves along the desired path ahead of the aircraft. The two display parameters examined are the field of view of the picture (from $\pm 5^\circ$ to $\pm 45^\circ$ ) and the distance to the box (from 92 m (300 ft) to 6100 m (20 000 ft)). The results show that the pilots prefer a distance to the box of 915 m (3000 ft) and a field of view of $\pm 30^\circ$ . The best performance, both in the sense of quickness of error correction and lowest standard deviation, is obtained with a distance to the box of 92 m (300 ft) and a field of view of $\pm 15^\circ$ . A pilot-model analysis is used to determine the gains used by the pilots and the servomechanism-response characteristics of the pilot-aircraft-display system.					
17. Key Words (Suggested by Author(s)) Pictorial landing display Computer-derived display Cathode-ray-tube display format Pilot-model analysis			18. Distribution Statement  Unclassified - Unlimited  Subject Category 06		
19. Security Classif. (of this report) Unclassified	20. Security Classif. (of this page) Unclassified	21. No. of Pages 50	22. Price A03		